© 2015. Published by The Company of Biologists Ltd | The Journal of Experimental Biology (2015) 218, 388-403 doi:10.1242/jeb.112250

RESEARCH ARTICLE

# The proteomic response of cheliped myofibril tissue in the eurythermal porcelain crab *Petrolisthes cinctipes* to heat shock following acclimation to daily temperature fluctuations

**Michael A. Garland[1], Jonathon H. Stillman[2] and Lars Tomanek[1,*]**

## ABSTRACT

The porcelain crab *Petrolisthes cinctipes* lives under rocks and in mussel beds in the mid-intertidal zone where it experiences immersion during high tide and saturating humid conditions in air during low tide, which can increase habitat temperature by up to 20°C. To identify the biochemical changes affected by increasing temperature fluctuations and subsequent heat shock, we acclimated *P. cinctipes* for 30 days to one of three temperature regimes: (1) constant 10°C, (2) daily temperature fluctuations between 10 and 20°C (5 h up-ramp to 20°C, 1 h down-ramp to 10°C) and (3) 10–30°C (up-ramp to 30°C). After acclimation, animals were exposed to either 10°C or a 30°C heat shock to analyze the proteomic changes in claw muscle tissue. Following acclimation to 10–30°C (measured at 10°C), enolase and ATP synthase increased in abundance. Following heat shock, isoforms of arginine kinase and glycolytic enzymes such as aldolase, triose phosphate isomerase and glyceraldehyde 3-phosphate dehydrogenase increased across all acclimation regimes. Full-length isoforms of hemocyanin increased abundance following acclimation to 10–30°C, but hemocyanin fragments increased after heat shock following constant 10°C and fluctuating 10–20°C, possibly playing a role as antimicrobial peptides. Following constant 10°C and fluctuating 10–20°C, paramyosin and myosin heavy chain type-B increased in abundance, respectively, whereas myosin light and heavy chain decreased with heat shock. Actin-binding proteins, which stabilize actin filaments (filamin and tropomyosin), increased during heat shock following 10–30°C; however, actin severing and depolymerization proteins (gelsolin and cofilin) increased during heat shock following 10–20°C, possibly promoting muscle fiber restructuring. RAF kinase inhibitor protein and prostaglandin reductase increased during heat shock following constant 10°C and fluctuating 10–20°C, possibly inhibiting an immune response during heat shock. The results suggest that ATP supply, muscle fiber restructuring and immune responses are all affected by temperature fluctuations and subsequent acute heat shock in muscle tissue. Furthermore, although heat shock after acclimation to constant 10°C and fluctuating 10–30°C showed the greatest effects on the proteome, moderately fluctuating temperatures (10–20°C) broadened the temperature range over which claw muscle was able to respond to an acute heat shock with limited changes in the muscle proteome.

**KEY WORDS: Actin-binding proteins, ATP-buffering, Claw muscle, Energy metabolism, Immune response, Proteomics, Systems biology**

[1]California Polytechnic State University, Department of Biological Sciences, Center for Coastal Marine Studies, Environmental Proteomics Laboratory, 1 Grand Avenue, San Luis Obispo, CA 93407-0401, USA. [2]Romberg Tiburon Center for Environmental Studies, San Francisco State University, 3152 Paradise Drive, Tiburon, CA 94920-1205, USA.

*Author for correspondence (ltomanek@calpoly.edu)

**Received 11 August 2014; Accepted 8 December 2014**

## INTRODUCTION

Environmental temperature has a ubiquitous effect on rates of biochemical reactions and cellular structures in ectothermic organisms, which have adapted their cellular processes and structures to cope with the specific thermal properties of their habitat (Somero, 2012; Tomanek, 2010). An organism's ability to adjust biochemical processes to different body temperatures is in large part determined by the rate and amplitude of temperature change and its evolutionary history, e.g. the thermal environment it occupies and recent thermal history, e.g. acclimatization. For example, intertidal organisms show different physiological responses to heat stress during emersion and immersion as a result of differing heating rates under each condition (Bjelde and Todgham, 2013; Tomanek and Somero, 2000) and closely related species occupying environments that vary greatly in thermal fluctuations along the physical gradient from the subtidal to the mid-intertidal zone differ in their ability to adjust cardiac thermal performance and heat-shock protein synthesis in response to temperature acclimation (Stillman, 2003; Tomanek and Somero, 1999). However, although we have a good understanding of the thermal range of organisms and their physiological plasticity in response to constant temperatures and acute heat stress, very little is known about how daily temperature fluctuations affect the physiology of organisms and determine the response to a subsequent acute heat stress.

Studies on the intertidal mussel *Mytilus* show that acclimation to fluctuating temperatures broadens the range over which metabolic rate is temperature-independent and that temperature range of filtration-feeding is expanded in comparison to animals acclimated to constant temperatures (Widdows, 1976). A study on the response of the water flea (*Daphnia pulex*) to various temperature fluctuations (15°C, 15–25°C and 15–30°C daily) showed that the greatest fluctuations reduced metabolic rates after six generations but increased temperature tolerance after over 15 generations (Chen and Stillman, 2012). Thus, greater fluctuations come with increased physiological costs but also increased stress tolerance, suggesting a trade-off between the two. The evolutionary adaptations to differences in temperature fluctuations are largely unknown, although a study on gammarid amphipods showed greater molecular diversity in myosin isoforms in congeners from thermally more variable environments (Rock et al., 2009). A study on the transcriptomic changes in liver tissue of annual killifish (*Austrofundulus limnaeus*) in response to constant and fluctuating daily temperatures showed that genes involved in cell growth and proliferation, molecular and chemical chaperones and maintenance of membrane integrity differ between these conditions, providing a framework for the cellular processes that might be affected by temperature fluctuations (Podrabsky and Somero, 2004). To our knowledge there has not been a study of the proteomic changes that might occur under fluctuating temperature regimes, especially not



The Journal of Experimental Biology

The Journal of Experimental Biology (2015) doi:10.1242/jeb.112250

**List of abbreviations**

| | |
|---|---|
| IPG | immobilized pH gradient |
| $LT_{50}$ | median lethal temperature |
| MALDI | matrix-assisted laser desorption/ionization |
| MS/MS | tandem mass spectrometry |
| PCA | principal component analysis |
| PCAD | porcelain crab array database |
| pI | isoelectric point |
| PMF | peptide mass fingerprint |
| $S_1$ | slow twitch muscle fiber |
| $S_2$ | slow phasic muscle fiber |
| ToF-ToF | tandem time of flight |

for intertidal organisms that are typically experiencing greatly fluctuating thermal conditions.

Proteomic analyses of non-model organisms have become possible recently because of the increasing number of completed genome sequences and well-annotated expressed sequence tag (EST) libraries and have added to our understanding of the responses of marine organisms to temperature, osmotic, hypoxic and oxidative stress (Tomanek, 2011; Tomanek, 2014). Specifically, a number of recent proteomic analyses of gill tissue of several marine non-model organisms in response to acute heat and chronic warm temperature stress showed that temperature stress increases the abundance of oxidative stress proteins and molecular chaperones, presumably because of the effect of reactive oxygen species on the cytoskeleton (Dilly et al., 2012; Fields et al., 2012a; Fields et al., 2012b; Tomanek and Zuzow, 2010). However, how temperature fluctuations affect the proteomic response to heat stress is not known.

Species of the porcelain crab genus *Petrolisthes* are distributed from the shallow subtidal to mid-intertidal zone of rocky shores where they experience temperature fluctuations of up to 20°C during a tidal cycle under conditions that range from submersion to fully humid (Teranishi and Stillman, 2007). Furthermore, the trancriptome of several tissues of one species, *Petrolisthes cinctipes*, has been characterized in response to acute temperature stress (Tagmount et al., 2010; Teranishi and Stillman, 2007). *Petrolisthes cinctipes* occupies the mid- to high-intertidal zone and has one of the highest thermal tolerances of the temperate *Petrolisthes* congeners (Stillman and Somero, 2000). In addition, it shows limited adjustments in thermal limits, e.g. $LT_{50}$, with increasing acclimation temperature, in contrast to its subtidal to low-intertidal temperate congeners (Stillman, 2003). Thus, given the thermal biology of *P. cinctipes* and with the transcriptomic database as a foundation for the identification of proteins with mass spectrometry, we assessed how the proteome of claw muscle tissue changes during acclimation to three different ranges of temperature fluctuations and a subsequent heat stress. Our results suggest that different ranges of thermal fluctuations affect energy metabolism, oxygen delivery, actomyosin structures and dynamics and the immune response of claw muscle tissue during subsequent heat stress.

## RESULTS AND DISCUSSION

We generated a fused image comprising gels from all temperature acclimation and acute heat shock treatments. In this fused gel image (Fig. 1), we detected 469 protein spots. Of these spots, 42% (197) changed abundance in response to temperature acclimation, acute heat shock, or their interaction; functional annotations were available for 73.6% (145) of these proteins (supplementary material Table S1). Changes in protein abundance may be attributed to an increase or decrease in synthesis, degradation or post-translational modifications (PTMs), including partial proteolysis. Thus, our interpretation is based on a subset of protein isoforms, which might not represent the full complement of isoforms of a particular protein and therefore might not represent the complete abundance of this protein. With these limitations in mind, our interpretations are meant to be hypotheses that generally require further validation.

To discuss the contribution of the cellular processes associated with the function of specific proteins, we grouped proteins into the following categories: ATP buffering, energy metabolism, respiratory, cytoskeletal and signaling proteins. Cytoskeletal proteins were separated into thin filament (actins), thick filament (myosins) and actin-binding proteins.

### Principal component analysis

We conducted principal component analyses (PCAs) to assess the variation in protein abundance patterns based on statistical significance for acclimation, heat shock or interaction effects, based on a two-way permutation ANOVA ($P \leq 0.02$). Principal components

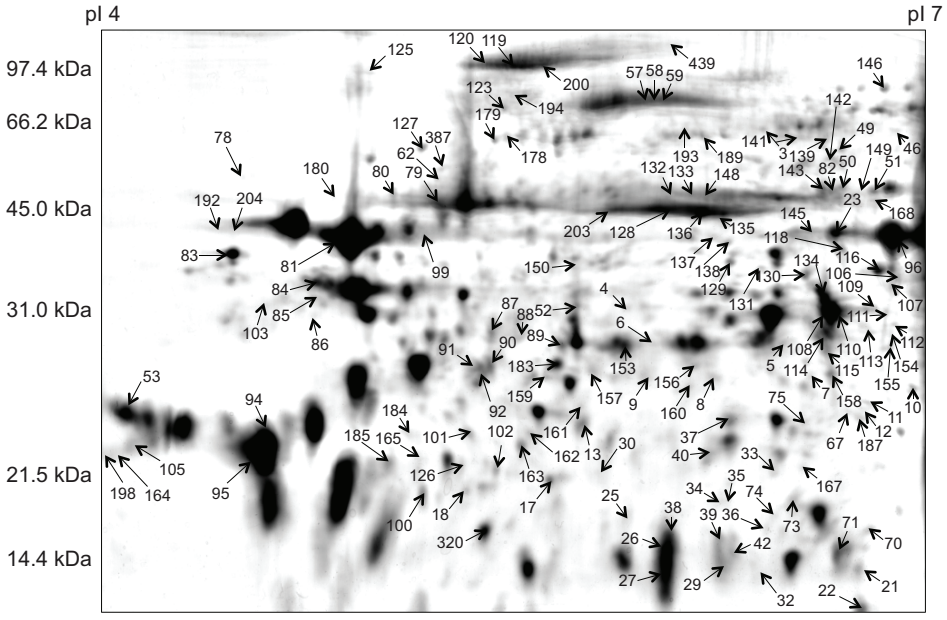


**Fig. 1. Proteome map of gels from all six treatments depicting 469 protein spots from claw muscle tissue of the intertidal porcelain crab *Petrolisthes cinctipes*.** The proteome map represents average pixel volumes for each protein spot. Numbered spots are those that changed abundance in response to acclimation and heat stress treatments (two-way permutation ANOVA; $P \leq 0.02$) and were identified using tandem mass spectrometry (for identification, see supplementary material Table S1).

The Journal of Experimental Biology (2015) doi:10.1242/jeb.112250

(PCs) that separated the treatments were analyzed further by identifying proteins that contributed the most to the separation, based on their loadings.

The first PCA (Fig. 2A) includes 83 proteins (65 identified) that were significant for an acclimation effect. The first component (PC1; 30.5%), separated both 10–30°C acclimation treatments (positive values on *x*-axis) from all other treatments. The second component (PC2; 16.4%) represented the effect of 10°C and 10–30°C acclimation regimes on a subsequent heat shock (negative values on *y*-axis). Heat shock following the 10–20°C acclimation only had a limited effect on shifting samples along PC2, suggesting that these temperature fluctuations induced a cellular response that prepared the animals for

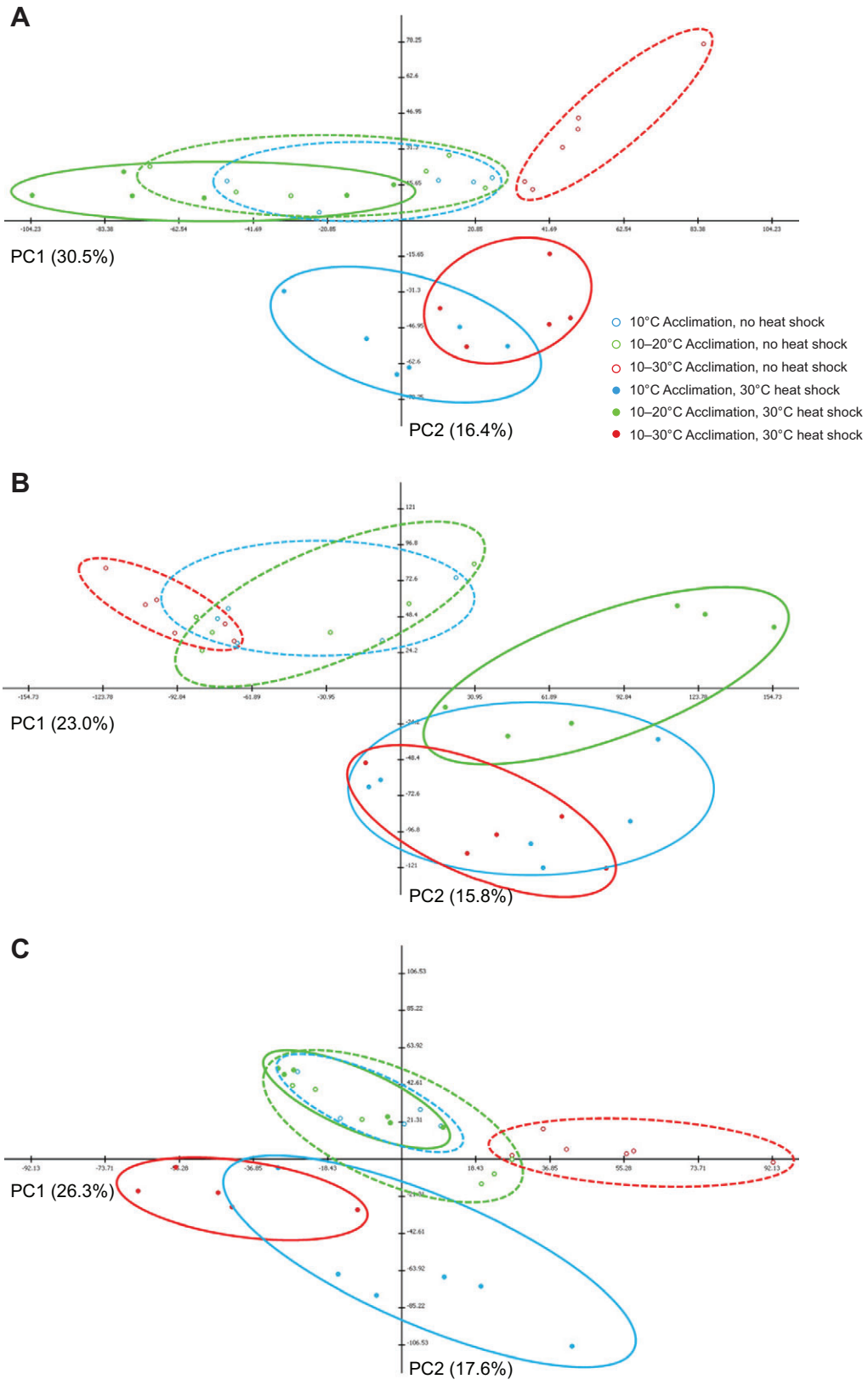


**Fig. 2. Principal component analysis (PCA) of treatments based on proteins that showed a significant acclimation, heat shock or interaction effect.** (A) acclimation, (B) heat shock and (C) interaction effect (based on a two-way permutation ANOVA; $P \leq 0.02$). Each symbol represents a crab acclimated to 10°C (blue), 10–20°C (green) and 10–30°C (red) and either subsequently exposed to 10°C (striated) or a 5 h up-ramp to a 30°C heat shock plus a 1 h down-ramp 10°C recovery (solid line) (samples collected after recovery at 10ºC). Principal components 1 and 2 (PC1 and PC2) and the percentage of the total variation of the selected (significant protein) data set they explain are shown. See text for explanation of PC1 and PC2 for each PCA.

The Journal of Experimental Biology (2015) doi:10.1242/jeb.112250

**Table 1. Positive and negative loadings for principal components 1 and 2 of proteins significant for an acclimation effect**

| Component loading rank | Principal component 1 | | Principal component 2 | |
|---|---|---|---|---|
| | Protein (spot ID) | Loading value | Protein (spot ID) | Loading value |
| Positive loadings for acclimation effect | | | | |
| 1 | Gelsolin (18) | 1.3186 | Enolase (50) | 1.4194 |
| 2 | Hemocyanin (37) | 1.2507 | Phosphoglycerate kinase (143) | 1.3506 |
| 3 | Arginine kinase (5) | 1.2112 | Enolase (149) | 1.2628 |
| 4 | Fructose 1,6-bisphosphate aldolase (320) | 1.2073 | Arginine kinase (23) | 1.2576 |
| 5 | Cardiac-like muscle actin (29) | 1.2030 | Muscle myosin heavy chain (120) | 1.2374 |
| 6 | Myosin heavy chain type B (71) | 1.1539 | Enolase (51) | 1.2247 |
| 7 | Hemocyanin subunit 1 (160) | 1.1395 | Hemocyanin (58) | 1.0674 |
| 8 | α/β-Actin (84) | 1.0984 | α/β-Actin (82) | 1.0664 |
| 9 | Arginine kinase (100) | 1.0963 | Hemocyanin (59) | 1.0536 |
| 10 | α/β-Actin (85) | 1.0526 | Arginine kinase (145) | 0.9337 |
| Negative loadings for acclimation effect | | | | |
| 1 | Gelsolin (18) | –1.6349 | Arginine kinase (109) | –2.1154 |
| 2 | Hemocyanin (37) | –1.5935 | Arginine kinase (102) | –2.0273 |
| 3 | Arginine kinase (5) | –1.5332 | Notch-type protein (139) | –1.9344 |
| 4 | Fructose 1,6-bisphosphate aldolase (320) | –1.5319 | Filamin-C (141) | –1.9090 |
| 5 | Cardiac-like muscle actin (29) | –1.5179 | Filamin-A (142) | –1.8065 |
| 6 | Myosin heavy chain type B (71) | –1.5089 | Arginine kinase (116) | –1.7500 |
| 7 | Hemocyanin subunit 1 (160) | –1.4944 | Filamin-A (46) | –1.7448 |
| 8 | α/β-Actin (84) | –1.4927 | α/β-Actin (39) | –1.6239 |
| 9 | Arginine kinase (100) | –1.4520 | Arginine kinase (107) | –1.6090 |
| 10 | α/β-Actin (85) | –1.4032 | Arginine kinase (114) | –1.4448 |

Compare table with results in Fig. 2A.

a 30°C heat shock, requiring limited changes of the proteome. The 10°C and 10–30°C acclimation regimes did not do the same. Thus, moderate temperature fluctuations broadened the range over which the claw muscle could respond to heat stress.

Proteins representing ATP buffering (arginine kinase), glycolysis (phosphoglycerate kinase and enolase) and thin (actin) filaments showed the most positive loadings (indicating greater abundances in the 10–30°C acclimation group; Table 1). ATP buffering and thin filament proteins also contributed highly negative loadings (lower abundances in the 10–30°C acclimation), suggesting that these functions changed the most with the most extreme daily temperature fluctuations. Interestingly, whereas some glycolytic proteins showed highly positive loadings (phosphoglycerate kinase and enolase), others showed highly negative loadings (fructose 1,6-bisphosphate aldolase or aldolase) for PC1, suggesting differences between the preparatory and the pay-off phase of glycolysis. Similarly, although some full-length hemocyanins showed highly positive loadings (spots 58 and 59), others that are fragments of the full-length protein (spots 37 and 160) showed negative loadings, suggesting that full-length hemocyanin increased whereas fragments decreased in the 10–30°C acclimation (see below).

PC2 separated the 10°C and 10–30°C heat shock treatments from all others. The pay-off phase of glycolysis and ATP buffering contributed the most to the positive loadings (Table 1), similar to PC1. ATP buffering (five arginine kinase isoforms) and actin-binding proteins (three filamin isoforms) contributed the most to the negative loadings (higher abundances at 10°C heat shock and 10–30°C heat shock). Additionally, a neurogenic notch homolog played a role during heat shock.

The PCA based on proteins that significantly changed with acute heat shock included 130 (90 identified) proteins (Fig. 2B). The heat shock treatments of all three acclimation regimes are separated along PC1 (23%; positive) and PC2 (15.8%; negative).

Glycolysis (glyceraldehyde 3-phosphate dehydrogenase or GAPDH), ATP-buffering, thin filaments and respiratory (or antimicrobial – see below) proteins (hemocyanin fragments) contributed highly positive loadings to PC1, with higher abundances following heat shock (Table 2). Four myosin heavy chain (three type B) isoforms contributed highly positive loadings. The negative loadings of respiratory proteins (full-length hemocyanins) and thick filaments (myosin non-type-B) along PC1 coincided with lower abundances during heat shock. The role of prostaglandin reductase, which showed the second highest positive loading along PC1, might be to suppress inflammation during heat shock (see below).

Along PC2, positive loadings by four myosin regulatory light chain isoforms coincided with lower abundances during heat shock. Combined with the loadings for PC1, it seems that heat shock leads to higher abundances of myosin heavy chain (type B and non-type B) but lower abundances of different myosin regulatory heavy and light chain isoforms. Negative loadings of three filamins, an actin-binding protein that connects actin filaments (van der Flier and Sonnenberg, 2001), along PC2 were based on higher abundances during heat shock following the 10°C and 10–30°C acclimation regimes. Thus, heat shock leads to higher abundances of myosin heavy chain (but lower abundances of myosin regulatory light chain and distinct heavy chain isoforms), hemocyanin fragments (spots 12 and 138), filamins and arginine kinase isoforms.

Seventy-one proteins (55 identified) contributed significantly to the interaction effect (Fig. 2C). PC1 (26.3%) separated the control (most positive) and the heat shock (most negative) treatments of the 10–30°C acclimation regime the most. PC2 (17.6%) separated the 10°C acclimation plus heat shock (most negative) from all other treatments. In contrast, 10–20°C acclimation control and 10–20°C acclimation control plus heat shock overlapped, again suggesting that moderate temperature fluctuations broaden the range over which claw muscle can respond to an acute heat stress. More specifically, several thin filament and respiratory proteins (most positive loadings) increased with acclimation to 10–30°C, whereas ATP buffering and thin and thick (myosin heavy chain) filament proteins (most negative loadings) increased with 10–30°C plus heat shock (Table 3). Also, full-length hemocyanins increased under the 10–30°C acclimation regime under control, but not acute heat shock.

The Journal of Experimental Biology (2015) doi:10.1242/jeb.112250

**Table 2. Positive and negative loadings for principal components 1 and 2 of proteins significant for a heat shock effect**

| Component loading rank | Principal component 1 | | Principal component 2 | |
|---|---|---|---|---|
| | Protein (spot ID) | Loading value | Protein (spot ID) | Loading value |
| Positive loadings for heat shock effect | | | | |
| 1 | GAP dehydrogenase (8) | 1.9067 | Sarcoplasmic $Ca^{2+}$-binding protein (95) | 1.7940 |
| 2 | Prostaglandin reductase (30) | 1.8708 | Myosin regulatory light chain (105) | 1.4420 |
| 3 | Arginine kinase (4) | 1.8526 | α/β-Actin (85) | 1.3084 |
| 4 | α/β-Actin (185) | 1.8511 | Myosin regulatory light chain (53) | 1.2316 |
| 5 | Myosin heavy chain type B (71) | 1.8142 | Myosin regulatory light chain (164) | 1.0045 |
| 6 | Muscle myosin heavy chain (126) | 1.7344 | Myosin regulatory light chain (198) | 0.8680 |
| 7 | Hemocyanin (12) | 1.7327 | Arginine kinase (7) | 0.8186 |
| 8 | Myosin heavy chain type B (26) | 1.7262 | α/β-Actin (78) | 0.8182 |
| 9 | Peroxiredoxin 5 isoform B (11) | 1.7057 | Myosin heavy chain type B (38) | 0.7772 |
| 10 | Myosin heavy chain type B (38) | 1.6357 | Arginine kinase (110) | 0.7329 |
| Negative loadings for heat shock effect | | | | |
| 1 | Hemocyanin (58) | –1.6951 | Filamin-C (141) | –2.2402 |
| 2 | Hemocyanin (57) | –1.6464 | Filamin-A (142) | –2.1902 |
| 3 | Troponin T (133) | –1.6351 | Notch-type protein (139) | –2.1898 |
| 4 | Muscle myosin heavy chain (119) | –1.6135 | Filamin-A (46) | –2.0921 |
| 5 | Myosin heavy chain type 1 (200) | –1.6073 | Arginine kinase (109) | –2.0472 |
| 6 | Myosin regulatory light chain (96) | –1.6019 | Arginine kinase (102) | –2.0086 |
| 7 | α/β-Actin (132) | –1.5946 | Arginine kinase (111) | –2.0012 |
| 8 | Arginine kinase (110) | –1.5669 | Hemocyanin (138) | –1.9705 |
| 9 | Hemocyanin (59) | –1.5660 | Paramyosin (3) | –1.8089 |
| 10 | Cardiac-like muscle actin (148) | –1.5277 | Arginine kinase (116) | –1.7964 |

Compare table with results in Fig. 2B.

ATP buffering also contributed high negative loadings to PC2 by increasing abundances with heat shock following the 10°C acclimation. Thin and thick filaments contribute positive loadings, suggesting that some actins and myosin decreased abundance at 10°C acclimation plus heat shock. Two enolase isoforms showed positive loadings along PC2 (decreasing abundance with 10°C acclimation plus heat shock), whereas another glycolytic protein, GAPDH, showed highly negative loadings for PC2 (higher abundance with 10°C acclimation plus heat shock). This suggests that these glycolytic reactions are responding differently to heat shock following acclimation to 10°C: with a decrease and increase in abundance with heat shock for enolase and GAPDH, respectively. GAPDH also increases abundance with heat shock following the 10–30°C acclimation.

### Energy metabolism

The majority of metabolic proteins identified are either involved in the transfer of phosphoryl groups, e.g. arginine kinase, or in ATP

**Table 3. Positive and negative loadings for principal components 1 and 2 of proteins significant for an interaction (acclimation by heat shock) effect**

| Component loading rank | Principal component 1 | | Principal component 2 | |
|---|---|---|---|---|
| | Protein (spot ID) | Loading value | Protein (spot ID) | Loading value |
| Positive loadings for interaction effect | | | | |
| 1 | α/β-Actin (128) | 1.7323 | α/β-Actin (85) | 1.5237 |
| 2 | α/β-Actin (136) | 1.7158 | Sarcoplasmic $Ca^{2+}$-binding protein (95) | 1.4294 |
| 3 | Hemocyanin (58) | 1.6991 | α/β-Actin (78) | 0.9058 |
| 4 | α/β-Actin (79) | 1.6647 | Enolase (51) | 0.9041 |
| 5 | Hemocyanin (59) | 1.6032 | Cofilin (33) | 0.8396 |
| 6 | α/β-Actin (135) | 1.4906 | Slow muscle myosin S1 heavy chain (178) | 0.8298 |
| 7 | Hemocyanin (57) | 1.4780 | Arginine kinase (7) | 0.7623 |
| 8 | Cardiac-like muscle actin (122) | 1.4513 | Arginine kinase (113) | 0.7188 |
| 9 | Phosphoglycerate kinase (143) | 1.2923 | Enolase (50) | 0.6708 |
| 10 | Hemocyanin subunit 2 precursor (62) | 1.2545 | Muscle myosin heavy chain (120) | 0.5270 |
| Negative loadings for interaction effect | | | | |
| 1 | Arginine kinase (89) | –1.7986 | Arginine kinase (116) | –2.1995 |
| 2 | Cardiac-like muscle actin (42) | –1.4293 | GAP dehydrogenase (106) | –2.1973 |
| 3 | α/β-Actin (39) | –1.3576 | Arginine kinase (107) | –2.1907 |
| 4 | Myosin heavy chain type B(27) | –1.3297 | Notch-type protein (139) | –2.0801 |
| 5 | GAP dehydrogenase (73) | –1.2943 | Arginine kinase (109) | –1.8695 |
| 6 | Filamin-C (141) | –1.2213 | Filamin-A (46) | –1.8568 |
| 7 | α/β-Actin (92) | –1.1390 | Paramyosin (118) | –1.7689 |
| 8 | Slow muscle myosin S1 heavy chain (178) | –1.0188 | Troponin T (168) | –1.7318 |
| 9 | Arginine kinase (102) | –0.9598 | α/β-Actin (121) | –1.6839 |
| 10 | Arginine kinase (109) | –0.7862 | Arginine kinase (102) | –1.6388 |

Compare table with results in Fig. 2C.



The Journal of Experimental Biology

The Journal of Experimental Biology (2015) doi:10.1242/jeb.112250

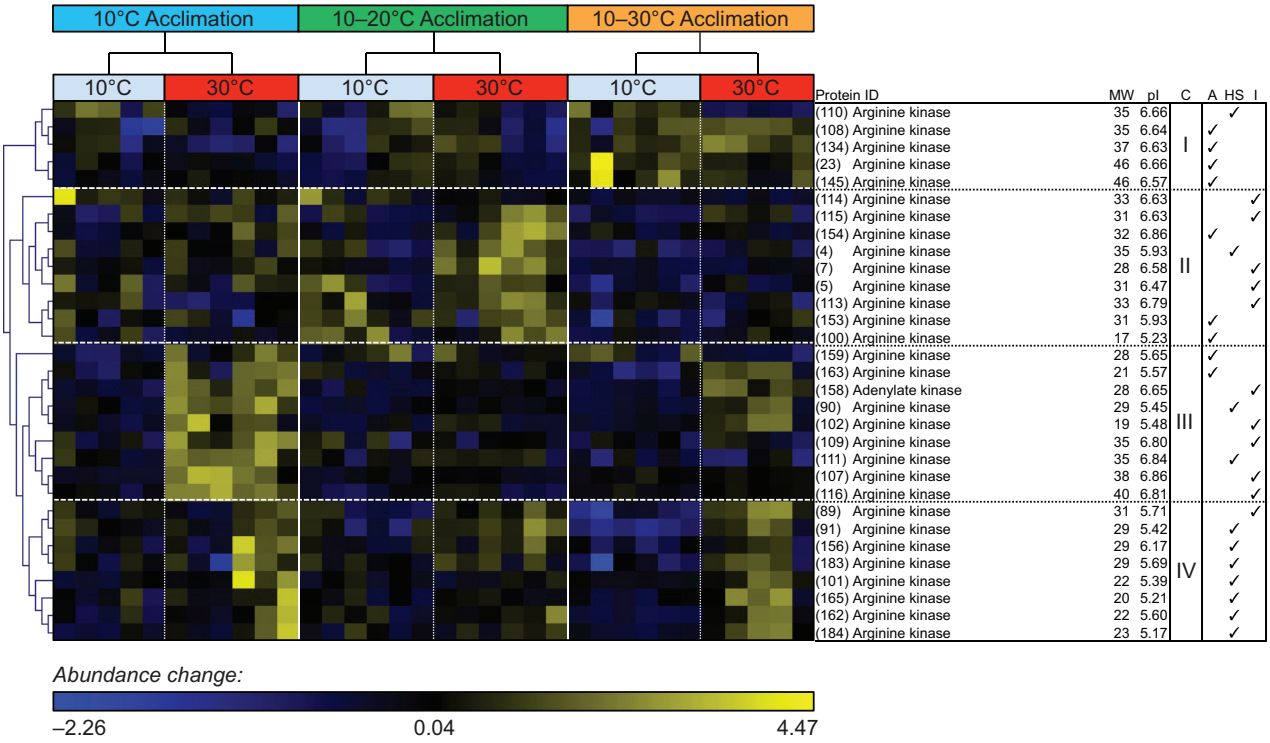


**Fig. 3. Hierarchical clustering of changes in abundance of phosphotransfer proteins.** Pearson's correlation, in response to acclimation to daily temperature fluctuations and subsequent control (10°C) and heat shock (30°C) exposures from claw muscle tissue of the porcelain crab *Petrolisthes cinctipes*. Blue coloring represents a lower than average protein abundance (standardized values, normalized volumes), whereas yellow represents greater than average protein abundance. Each column represents an individual muscle, grouped by treatment ($N$=5-6 for each treatment). The rows represent the standardized abundances of proteins, organized by clusters of similar abundance changes (C), that are identified to the right and whose molecular mass (MW) and isoelectric point (pI) is listed. Significances for an acclimation (A), heat shock (HS) or interaction (I) effect are ticked based on a two-way permutation ANOVA ($P$≤0.02).

production via glycolysis, e.g. GAPDH. We will first discuss them separately and then describe possible links.

### Phosphotransfer proteins

Thirty arginine kinase isoforms changed abundance and were separated into four general groups: those with high abundance following the 10–30°C acclimation (cluster I), high abundance following 10–20°C heat shock (and low abundance following 10–30°C; cluster II) and those with high abundance during heat shock following 10°C acclimation (and some isoforms following 10–30°C heat shock; cluster III) or all three acclimation treatments (cluster IV; Fig. 3). These groupings are generally supported by the statistical results, indicating significance for acclimation (clusters I and II) or heat stress (cluster IV) alone or an interaction effect (cluster III). The number of arginine kinase isoforms varied from five (cluster I) to nine.

The diversity of arginine kinase isoforms can, in part, be explained by the existence of four different arginine kinase transcripts in the *Petrolisthes* EST library (Tagmount et al., 2010). They may be separate isoforms for the cytosolic and mitochondrial compartment (Uda et al., 2006). Although no post-translational modifications have been reported for arginine kinase, it is possible that arginine kinase has similar post-translational modifications to its vertebrate functional homolog, creatine kinase, which include nitrosylated or glutathionylated thiol groups that are related to oxidative stress and can affect creatine kinase activity (Reddy et al., 2000; Wolosker et al., 1996). Glutathionylation of one protein cysteine residue reduces the pI by 0.5 pH units (Ubuka et al., 1987). Interestingly, several arginine kinase isoforms that increase abundance with heat shock (clusters III and IV) show lower pIs that are about one pH unit lower than the majority of arginine kinase isoforms of cluster I, possibly indicating two glutathionylation sites (Fig. 3). Claw tissue includes four muscle subtypes (dactyl, propodus, carpus and merus), but there is no evidence for muscle-specific arginine kinase isoforms. Another 2-D gel electrophoresis analysis on the prawn *Marsupenaeus japonicas* showed three isoforms increasing abundance in muscle tissue during recovery from hypoxic stress (Abe et al., 2007), suggesting that energetic stress causes changes in the abundance of multiple arginine kinase isoforms.

Given that the temperature fluctuations applied in our experiment probably affected reaction rates and therefore caused high and fluctuating ATP consumption rates, we assume that arginine kinase's main function under these circumstances is the transfer of phosphoryl groups from arginine phosphate to $MgADP^-$ to maintain ATP levels and thereby energy homeostasis (Ellington, 2001; Hochachka, 2003). However, arginine kinase also affects glycolytic rates through the release of inorganic phosphate, which serves as (1) a substrate for glycogen phosphorylase, leading to the breakdown of glycogen to glucose-1-phosphate, and (2) a $H^+$ buffer during glycogenolysis and glycolysis (Ellington, 2001; Griffiths, 1981). Support for a possible role of arginine kinase isoforms in regulating glycogenolysis comes from the identification of glycogen phosphorylase, which increased abundance with heat shock after acclimation to 10°C and 10–20°C (Fig. 4). Furthermore, glycogen phosphorylase is regulated by

The Journal of Experimental Biology (2015) doi:10.1242/jeb.112250

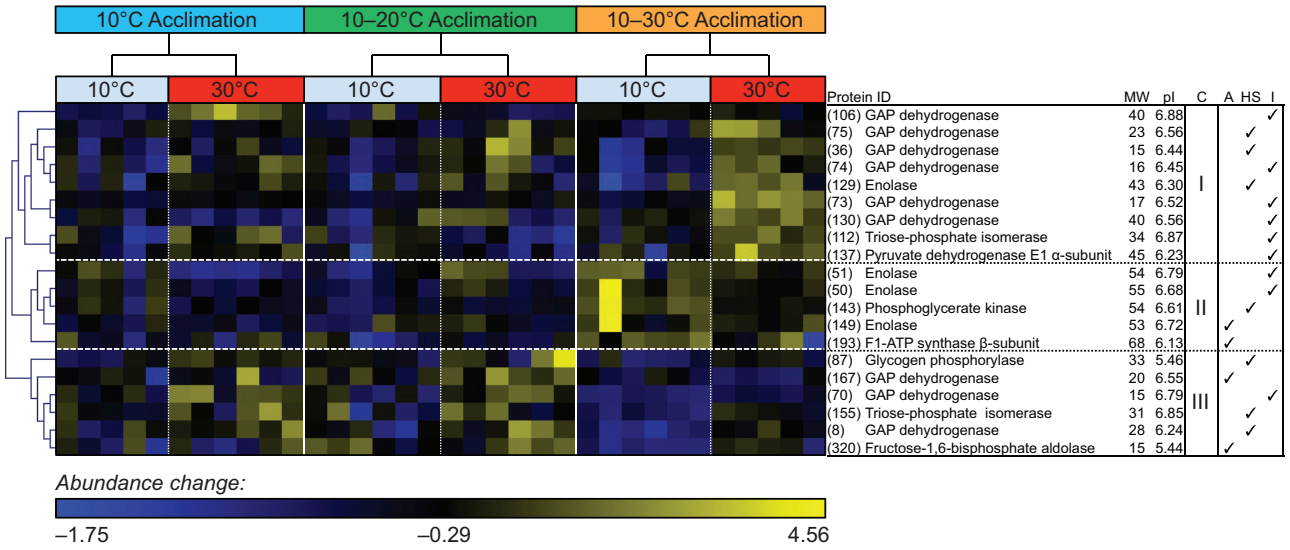


**Fig. 4. Hierarchical clustering of changes in abundance of proteins involved in energy metabolism.** Pearson's correlation, in response to acclimation to daily temperature fluctuations and subsequent control (10°C) and heat shock (30°C) exposures from claw muscle tissue of the porcelain crab *Petrolisthes cinctipes*. For additional details, see Fig. 3.

phosphorylation and, in addition, AMP levels [for an interesting historical account of this topic, see Fischer (Fischer, 2013)], which are regulated in part by adenylate kinase, which catalyzes the conversion of two ADP into ATP and AMP and showed an interaction effect (Fig. 3). Together these findings suggest an important role for ATP-buffering and glycogenolysis during heat shock after acclimation to constant 10°C and moderately fluctuating temperatures and a possible role for arginine and adenylate kinase in regulating these cellular pathways.

### Glycolysis

Most of the metabolic proteins that changed during acclimation and acute heat shock are part of the glycolytic pathway (Fig. 4). Acclimation to different thermal conditions, followed by a 30°C heat shock, led to three major clusters of protein abundances: cluster I showed increased abundances specifically during heat shock following the 10–30°C acclimation in nine protein isoforms. Six of the isoforms in this cluster were identified as GAPDH, one as triose phosphate isomerase (TPI), enolase and pyruvate dehydrogenase (PDH), respectively. Cluster II showed an increase in abundance of three enolase and one phosphoglycerate kinase isoforms during 10–30°C acclimation. Cluster III showed an increase in abundance by three enzymes, GAPDH (three isoforms), TPI and aldolase, during heat shock following acclimation to 10°C and 10–20°C. This cluster also includes glycogen phosphorylase. Thus, we have a cluster that is characterized by an increase in abundance with acclimation to 10–30°C (cluster II) and with heat shock following acclimation to 10–30°C (cluster I) and 10°C as well as 10–20°C (cluster III). Thus, the three reactions from fructose-1,6-bisphosphate to 1,3-bisphosphoglycerate, including aldolase, TPI and GAPDH, are potentially modified in response to acute heat shock (cluster III), possibly to support ATP production under acute stress conditions through glycolysis. Acclimation to constant daily fluctuations of 10–30°C led to an increase in three enolase isoforms, phosphoglycerate kinase and F1-ATP synthase β-subunit. The three isoforms of enolase differ mainly in pI but not mass, suggesting that they differ in post-translational modifications. These changes also affected the response to acute heat shock following acclimation to 10–30°C, increasing the abundance of five additional GAPDH isoforms, TPI and enolase, as well as PDH. Thus, the reactions of the triangle between aldolase, GAPDH and TPI characterize the response to acute heat shock following acclimation to constant (10°C) and moderate temperature fluctuations (10–20°C), but more extreme fluctuations require several additional enolase and GAPDH isoforms and phosphoglycerate kinase.

A possible explanation for the number of enolase and GAPDH isoforms are post-translational modifications, e.g. glutathionylation, which is known to modify and affect the activity of GAPDH, TPI and aldolase (Dalle-Donne et al., 2009; Fratelli et al., 2003). In addition, enolase is modified by phosphorylation, acetylation and methylation (Zhou et al., 2010).

### Energy metabolism conclusions

The prominence of arginine kinase and glycolytic protein isoforms, e.g. GAPDH, in the proteomic responses to temperature acclimation and heat shock suggest an important role for phosphotransfer proteins and glycolysis in maintaining energy homeostasis in muscle tissue during temperature fluctuations. Creatine kinase (and by extension arginine kinase as well as adenylate kinase) and GAPDH (and phosphoglycerate kinase) are recognized as playing a role in providing an efficient intracellular network that couples ATP-consuming with ATP-producing processes based on near-equilibrium metabolic reactions, thereby improving the efficiency of the transfer of phosphoryl groups, specifically in cardiac muscle tissue (Dzeja and Terzic, 2003). The proteomic fingerprint we identified suggests that such a network exists in claw muscle and that it is modified during temperature fluctuations and acute heat shock conditions that temporarily demand high ATP turnover. This further suggests that the energetics of temperature acclimation are dependent on the restructuring of the cellular architecture, specifically the microstructure of those networks that are able to maintain ATP concentrations despite greatly fluctuating rates of ATP consumption (Hochachka, 2003).

### Hemocyanin

We identified eleven isoforms of hemocyanin, an oxygen-carrying protein of arthropods and molluscs (Burmester, 2001). In addition to its role as oxygen-carrier, hemocyanins have been shown to

The Journal of Experimental Biology (2015) doi:10.1242/jeb.112250

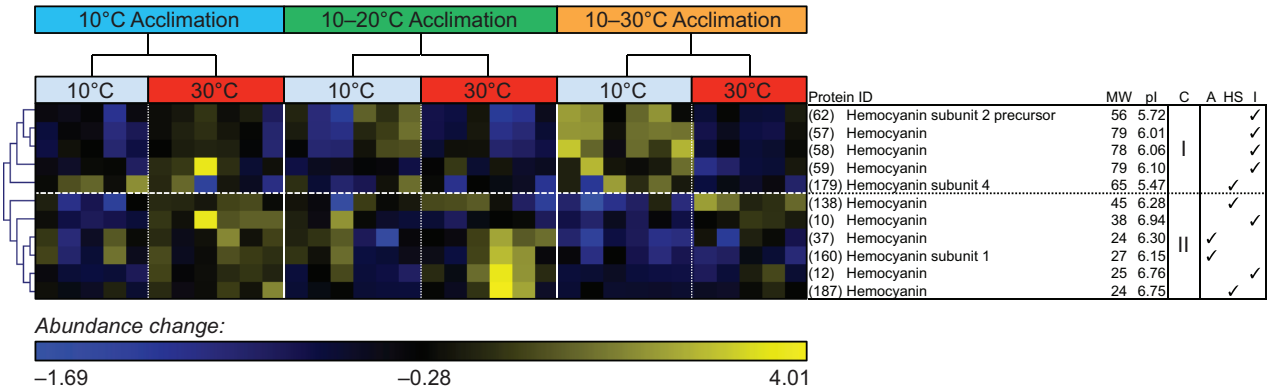


**Fig. 5. Hierarchical clustering of changes in abundance of hemocyanin isoforms.** Pearson's correlation, in response to acclimation to daily temperature fluctuations and subsequent control (10°C) and heat shock (30°C) exposures from claw muscle tissue of the porcelain crab *Petrolisthes cinctipes*. For additional details, see Fig. 3.

undergo a transition to function as catechol oxidases under certain *in vivo* conditions, and thus play a role in the sclerotization of the crustacean post-molt exoskeleton (Decker and Jaenicke, 2004). Hemocyanins also function as antimicrobial peptides after the C-terminal end is cleaved off during infection (Destoumieux-Garzón et al., 2001; Lee et al., 2003).

Hierarchical clustering of the hemocyanin isoforms suggests two major clusters (Fig. 5). Cluster I represents five isoforms that showed higher abundances with acclimation to 10–30°C, whereas cluster II has six isoforms that increased with heat shock following 10°C and 10–20°C, including one isoform that increased with heat shock following acclimation to 10–30°C. All hemocyanin isoforms in cluster I had masses equal or greater than 65 kDa, representing the full-length sequence. In contrast, all six isoforms of cluster II had masses between 24 and 48 kDa, and higher pIs than isoforms from cluster I. An almost identical pattern of hemocyanin isoforms was observed in hemocytes of the Pacific white shrimp *Penaeus vannamei* upon virus infection (Chongsatja et al., 2007). Subsequent work showed that isoforms similar to those with low molecular mass in cluster II are peptides cleaved off the N-terminal hemocyanin sequence in white shrimp (Havanapan et al., 2009). Hemocyanin isoforms of intermediate mass (spots 62, 138 and 179) may represent peptides cleaved off the C-terminus and may be phosphorylated by the ERK1/2 MAP kinase signaling pathway (see below for link to inflammation), explaining the relatively low pI of two of these isoforms (Havanapan et al., 2009). Only one of these three isoforms increased with heat shock after 10–30°C (spot 138).

Thus, the majority of cluster I represents full-length hemocyanin isoforms that were most likely increasing abundance in response to extreme daily temperature fluctuations, possibly to supply more oxygen. Cluster II most likely represents N- and C-terminal peptides cleaved off from full-length hemocyanins.

## Cytoskeletal proteins

In myofibrillar tissue, cytoskeletal elements compose the sarcomeres that are involved in muscle contraction. We identified a number of cytoskeletal proteins changing in response to temperature fluctuations. We separated these proteins into three functional categories: thick filament (myosins), thin filament (actins) and actin-binding proteins.

### Thick filament proteins (myosins)

We identified 22 thick filament proteins, including isoforms of myosin heavy chain (MHC), myosin regulatory light chain (MLC) and paramyosin (Fig. 6). Whereas the N-terminus of MHCs and MLCs make up the head of the thick filament that forms cross-bridges with actin, the C-terminus of MHCs makes up the rod (Clark et al., 2002). Paramyosins are part of the core of the rod in invertebrates (Hooper et al., 2008; Squire, 2009).

The PCA showed that changes in thick filament proteins contribute greatly to variation in the heat shock effect (Table 2), and this is shown in their hierarchical clustering (Fig. 6). For example, proteins in cluster IV showed sharply decreasing abundances following acute heat shock, regardless of acclimation regime. This cluster contains five isoforms of the regulatory MLC with molecular masses between 20 and 24 kDa (with one exception), as predicted, and five MHC isoforms, which suggests that acute thermal stress might negatively affect modulation of sarcomeric power output and stabilization of the MHC tail region (Tohtong et al., 1995; VanBuren et al., 1994). Several MHC isoforms from cluster IV showed increased abundances during acclimation, especially to 10–30°C, and range in mass from 75 to 108 kDa, below the predicted mass of 205 kDa (Mykles, 1997), a mass above the mass range of our 2-D gels. Myosin fragments of this size have been identified to form during apoptosis, using 2-D gel electrophoresis (Suarez-Herta et al., 2000) and could be the result of a heat-activated increase in proteolytic activity of the proteasome (Mykles and Haire, 1991). However, the fact that these isoforms showed increased abundances with acclimation to greater temperature fluctuations and showed reduced abundances with heat shock, suggests that it is a chronic and not an acute temperature stress signal, leading to this fragmentation pattern. It seems unlikely that apoptosis was elevated at 10°C acclimation (relative to heat shock), but an increase with greater temperature fluctuations at control conditions (10°C) would be a reasonable hypothesis.

While cluster IV decreased in response to heat shock, abundances of proteins of clusters I, II and III increased with heat shock in an acclimation-dependent manner. All heat-shock-induced isoforms of MHC and paramyosin, which are known in decapod crustaceans to be indicative of fiber type (Medler et al., 2004), had masses below their predicted range. For some MHCs (cluster I and II), these were even lower than for the 10–30°C acclimation-induced MHC fragments (cluster IV), but they were also from a different MHC type, suggesting that they originated from a separate proteolytic target. Because these changes were heat-shock-specific, it is possible that these changes are indicative of the beginning of an increase in protein turnover for fiber type switching between fast twitch (F), slow twitch ($S_1$) and slow

The Journal of Experimental Biology (2015) doi:10.1242/jeb.112250

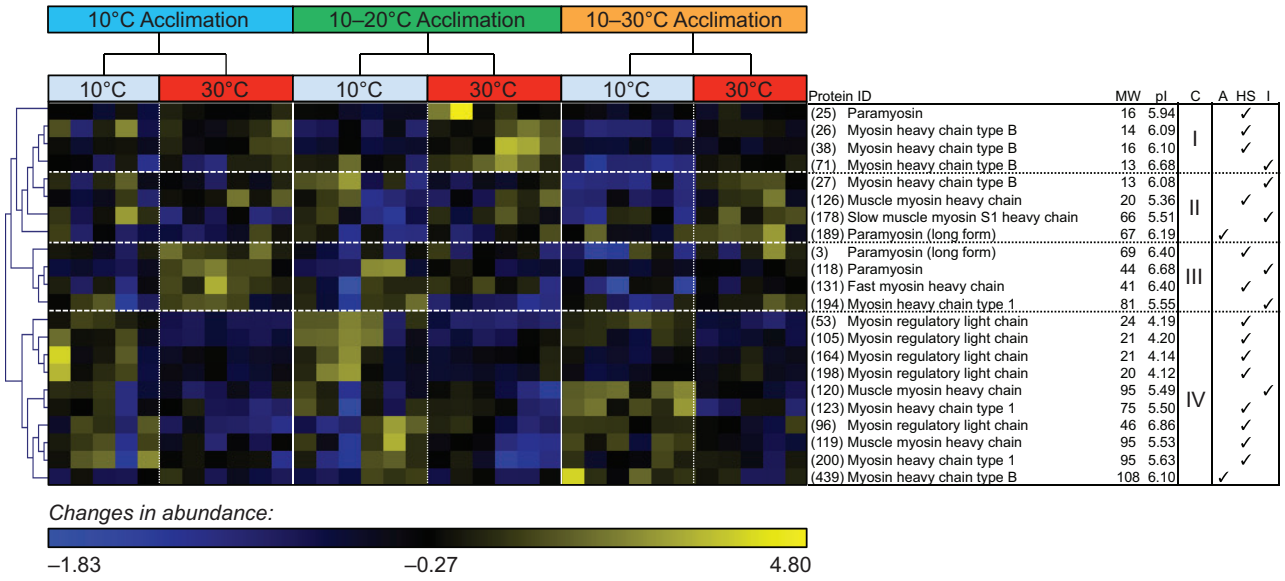


**Fig. 6. Hierarchical clustering of changes in abundance of thick filament proteins.** Pearson's correlation, in response to acclimation to daily temperature fluctuations and subsequent control (10°C) and heat shock (30°C) exposures from claw muscle tissue of the porcelain crab *Petrolisthes cinctipes*. For additional details, see Fig. 3.

phasic ($S_2$) in response to heat shock. In support of this hypothesis, the 10–30°C acclimation plus heat shock increased slow-twitch tropomyosin (see below), suggesting a shift to $S_1$ fiber type. Interestingly, gelsolin fragments, which are still able to sever actin filaments and represent an apoptotic signal (Kothakota et al., 1997), increased at 10–20°C acclimation plus heat shock (see below), possibly indicating that a 30°C heat shock following moderate temperature fluctuations causes a restructuring of the entire actomyosin complex.

### Thin filament proteins (actins)

Thin filaments are made of α- and β-actins and are the most abundant proteins in muscle tissue. We identified 30 different isoforms, with six cardiac-like muscle isoforms and 24 isoforms that are homologous to both α-actin of *Homarus americanus* and β-actin of *Scylla paramamosain*. In histochemical studies that examine crustacean actin, isoform diversity stems in part from tissue- and cellular-compartment-specific localization, including variants specific to the heart, skeletal muscle and cytoplasm (Varadaraj et al.,

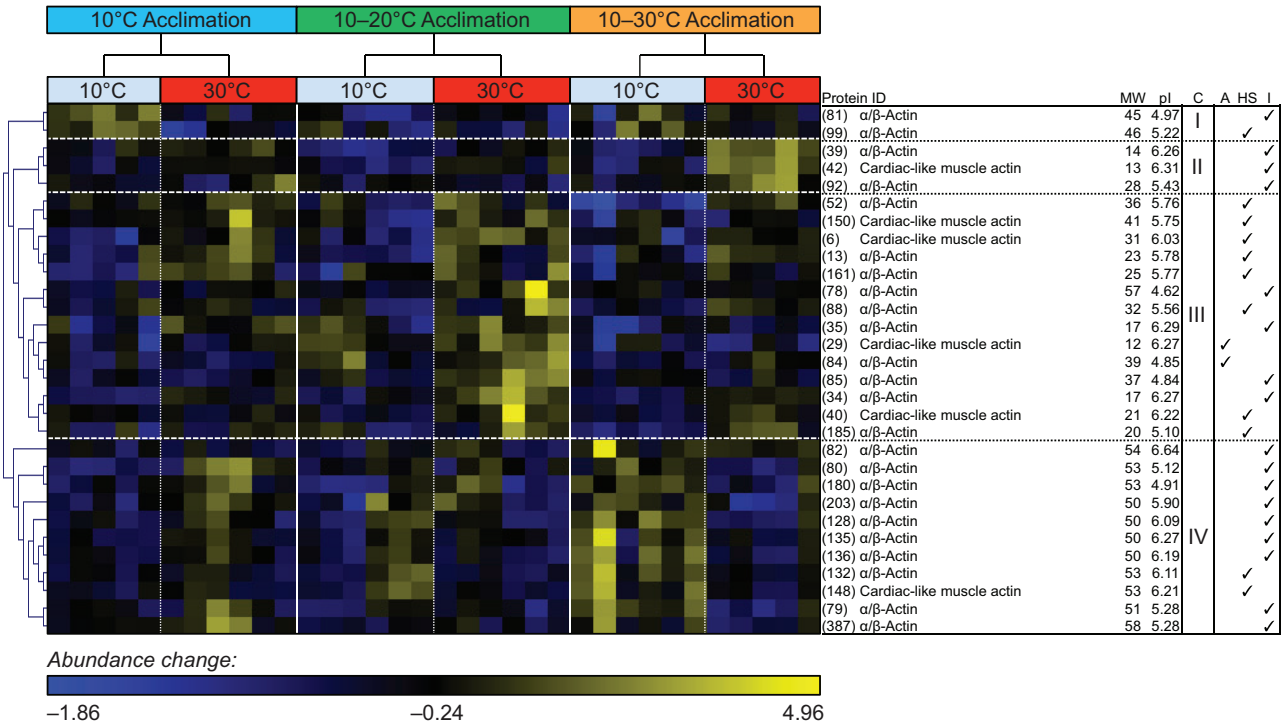


**Fig. 7. Hierarchical clustering of changes in abundance of thin filament proteins.** Pearson's correlation, in response to acclimation to daily temperature fluctuations and subsequent control (10°C) and heat shock (30°C) exposures from claw muscle tissue of the porcelain crab *Petrolisthes cinctipes*. For additional details, see Fig. 3.

1996; Kim et al., 2009). *Artemia* have at least 10 isoforms of actin, *Homerus americanus* has at least 12, and 8 have been found in *Gecarcinus lateralis* (Macias and Sastre, 1990; Ortega et al., 1992; Varadaraj et al., 1996; Kim et al., 2009). In the present study, we found 18 isoforms with a mass of at least 37 kDa, which is close to the predicted 42 kDa mass. The cytoskeleton is known to be involved in colocalization of energy metabolism enzymes and a separate study has verified this to be the case in *P. cinctipes* claw tissue (Götz et al., 1999; Cayenne et al., 2011). Changes in abundance can be grouped into four clusters that showed a regular correlation with patterns of molecular mass.

Cluster I showed increased abundances of two actin isoforms with a molecular mass of 45 and 46 kDa, close to the predicted 42 kDa, following acclimation to 10°C and 10–30°C (Fig. 7). Cluster II showed three isoforms with masses below 28 kDa with increased abundances after 10–30°C plus heat shock. Cluster III showed increased abundances following 10–20°C plus heat shock, with four cardiac muscle actins that ranged from 12 to 41 kDa, and ten α/β-actins with masses from 17 to 57 kDa, including five isoforms between 17 and 32 kDa, a mass range that is unlikely to represent a full-length isoform. Cluster IV showed increased abundances of 11 actin isoforms (one a cardiac-like muscle actin) ranging from 50 to 58 kDa after acclimation to 10–30°C.

We can divide the clusters into acclimation (I), heat shock (III) and interaction clusters (II and IV). Clusters II and III, which showed increased abundance of actin fragments, indicate partial *in vivo* proteolysis during heat shock. The fact that gels from non-heat-shock treatments did not show partial proteolysis suggests that the occurrence of fragments is not an artifact of our sample preparation protocol but is rather due to a low thermal stability intrinsic to actin, which depends on several actin-binding proteins and ATP levels, under *in vivo* conditions (Levitsky et al., 2008). Also, we observed a similar heat-shock-induced pattern of partial proteolysis for actin isoforms in sea squirts of the genus *Ciona* (Serafini et al., 2011).

### Actin-binding proteins

Actin-binding proteins (ABP) that regulate the dynamics of actin monomers and filaments also changed in abundance. They can be categorized into four groups: actin filament stabilizing (tropomyosin, Tm; filamin and sarcomeric α-actinin), severing and capping (gelsolins), G-actin binding proteins that regulate F-actin filament length (profilin and cofilin) and regulatory proteins (troponin T, TnT) (Clark et al., 2002; Lee and Dominguez, 2010). The protein isoforms we identified as belonging to these categories grouped into four clusters (Fig. 8).

Although 10°C acclimation plus heat shock led to an increase in most ABP (with cofilin and tropomyosin being the exceptions) across several clusters, cluster I was also characterized by increased abundances of cofilin (or actin depolymerization factor), the actin-severing protein gelsolin, the anchoring protein α-actinin and troponin T, which organizes the actin filament regulatory complex (Clark et al., 2002), following 10–20°C acclimation plus heat shock. Thus, we hypothesize that chronic moderate temperature fluctuations plus heat shock sever and depolymerize actin filaments and thereby activate actin filament restructuring (Lee and Dominguez, 2010). Moderate temperature fluctuations may also strengthen anchoring of filaments to the Z-line through α-actinin. Interestingly, this cluster coincides with an increase in the number of actin fragments (Fig. 7; cluster III).

Cluster II is the 10–30°C acclimation cluster with increased abundances of filamin, gelsolin and troponin (Fig. 8). The functions involve anchoring or bundling of actin filaments, severing and regulation of the tropomyosin–actin interaction, respectively. Cluster III showed an increase in two of the three proteins of the cluster, filamin and profilin, at 10°C acclimation plus heat shock, suggesting the need for anchoring or bundling actin filaments and binding of monomeric actin to control actin filament growth.

All three actin-stabilizing proteins showed an increase in abundance following 10–30°C and heat shock in cluster IV. Tropomyosins stabilize filaments (Wegner, 1982), actinins anchor filaments to the Z-line in striated muscles (Clark et al., 2002), whereas filamins may anchor or bundle actin filaments (van der Flier and Sonnenberg, 2001). Interestingly, this cluster increased abundances in response to an acute heat shock but not the 10–30°C acclimation and thus represents a strategy to stabilize actin filaments during acute heat shock only. Actinin and filamins but not tropomyosin also increased in response to heat shock following the 10°C acclimation.

Overall, heat shock triggered increased abundances for ABP involved in stabilizing actin filaments following acclimation to 10°C and 10–30°C but not to 10–20°C, based on the abundance patterns of actinin (spot 127 only), several filamins, and tropomyosin

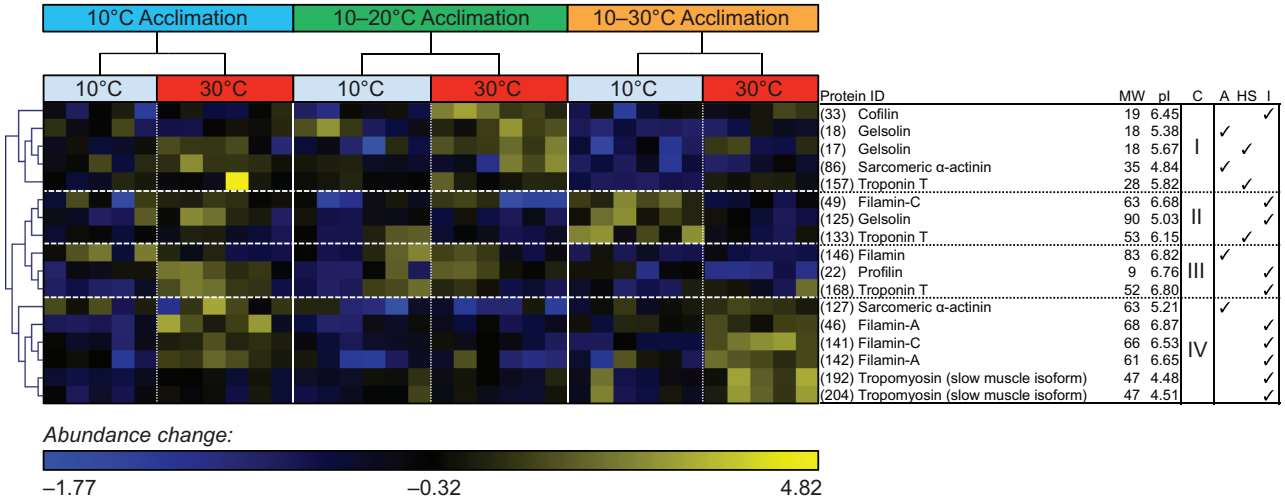


**Fig. 8. Hierarchical clustering of changes in abundance of actin-binding proteins.** Pearson's correlation, in response to acclimation to daily temperature fluctuations and subsequent control (10°C) and heat shock (30°C) exposures from claw muscle tissue of the porcelain crab *Petrolisthes cinctipes*. For additional details, see Fig. 3.

The Journal of Experimental Biology (2015) doi:10.1242/jeb.112250

(10–30°C plus heat shock only). Our interpretation suggests that acclimation to 10–20°C plus heat shock caused actin filament severing and depolymerization, based on changes in gelsolin and cofilin, respectively, and therefore limited actin filament growth and length. Three different troponin T isoforms were abundant following acclimation to 10°C, 10–20°C and 10–30°C plus heat shock, respectively. Troponin T anchors tropomyosin to the troponin trimer complex, and in conjunction with actin, is responsible for producing the 'swivel' effect in muscles (Myers et al., 1996; Murakami et al., 2008). Thereby, troponin T is thought to organize the regulatory complex of actin filaments (Clark et al., 2002). Finally, there is only one 10–30°C acclimation cluster (II) with high abundances of filamin C, gelsolin and troponin T, suggesting that chronic temperature fluctuations require increased bundling of actin filaments, greater rates of severing and modifications of the regulatory complex of the actomyosin interactions.

#### Thin filaments and actin-binding proteins

Thin filaments (actins) showed a much greater number of fragments at 10–20°C plus heat shock than at 10–30°C plus heat shock (Fig. 7, cluster III versus cluster II), indicating a greater resistance to partial proteolysis during heat shock following acclimation to 10–30°C. This pattern corresponds to increased abundances of actinin, which anchors actin to the Z-line (Clark et al., 2002; Wegner, 1982), tropomyosin, which stabilizes actin filaments (Clark et al., 2002; Wegner, 1982) and filamin, an actin-anchoring or actin-bundling protein (van der Flier and Sonnenberg, 2001) (Fig. 8; cluster IV). Thus, all three of these ABPs increased during heat shock following acclimation to 10–30°C only and possibly stabilized actin filaments and thereby reduced fragmentation. Thus, extreme but not moderate daily temperature fluctuations lead to an increase in proteins that stabilize actin filaments and enhance their anchoring to the Z-line and thereby possibly reduce fragmentation during acute heat shock.

In a pattern that complements the pattern of actin stabilization, the greater fragmentation of actin during heat shock following acclimation to 10–20°C is accompanied by increased abundances of cofilin (actin depolymerization factor), gelsolin, actinin and tropomyosin (Fig. 8; cluster I). At least in the case of cofilin and gelsolin, it seems likely that greater filament depolymerization and severing may increase the susceptibility of actin to partial proteolysis during heat shock. This is consistent with the observation that filamentous actin is much more thermally stable and therefore resistant to partial proteolysis than globular actin (Levitsky et al., 2008).

We hypothesize that acclimation to extreme temperature fluctuations (10–30°C) induces resistance to actin filament depolymerization and severing during heat shock (no increase in cofilin and gelsolin), in part through the greater thermal stability of filamentous versus globular actin. We further hypothesize that acclimation to mild temperature fluctuations (10–20°C) induces an increase in actin filament depolymerization and severing proteins during heat shock (30°C) and therefore greater G-actin formation, which, because G-actin is thermally more labile and supposedly unfolds more readily during heat shock, increases access to proteases and therefore increases partial proteolysis. It is unclear whether the putative greater sensitivity for increased filament severing under the 10–20°C acclimation plus heat shock conditions reflects a more dynamic actomyosin complex under control conditions, and whether greater filament stabilization following 10–30°C plus heat shock indicates a more rigid actomyosin complex under control conditions. We propose that actin filament dynamics may be undergoing adjustments, e.g. compensations, during temperature acclimation to maintain properties of the actomyosin complex similar to those known for enzyme activities and membrane fluidity (Hochachka and Somero, 2002).

### Signaling proteins

#### Calcium ion regulation

Changes in $Ca^{2+}$ concentration affect cellular processes, ranging from transcriptional activity in the nucleus to changes in muscle contraction in myofibrillar tissues (Clapham, 2007). In crustaceans, $Ca^{2+}$ regulation plays a key part in the molt cycle, depleting calcium from the $CaCO_3$ cuticle during proecdysis (pre-molt) and restoring it during the post-molt sclerotization process (Ahearn et al., 2004).

Sarcoplasmic $Ca^{2+}$-binding proteins (SCPs) belong to the family of EF-hand calcium-binding proteins and are found only among invertebrates (White et al., 2011; Gao et al., 2006; Hermann and Cox, 1995). We identified two isoforms of SCPs with estimated masses of 22 kDa (spot 94) and 21 kDa (spot 95). One isoform (spot 95) showed a lower level with heat shock after acclimation to 10°C and 10–30°C, the other one (spot 94) a decrease in abundance after acclimation to 10–20°C (Fig. 9). Spot 94 clusters with farnesoic acid O-methyltransferase and a notch homolog, possibly suggesting a role in inhibiting developmental processes during heat shock following the 10°C acclimation. Our MS/MS analysis identified the same three peptides for both SCP spots, and did not resolve why these SCPs have separate positions. Three SCP isoforms are possible splice variants in the freshwater crayfish *Procambrus clarkii* (White et al., 2011).

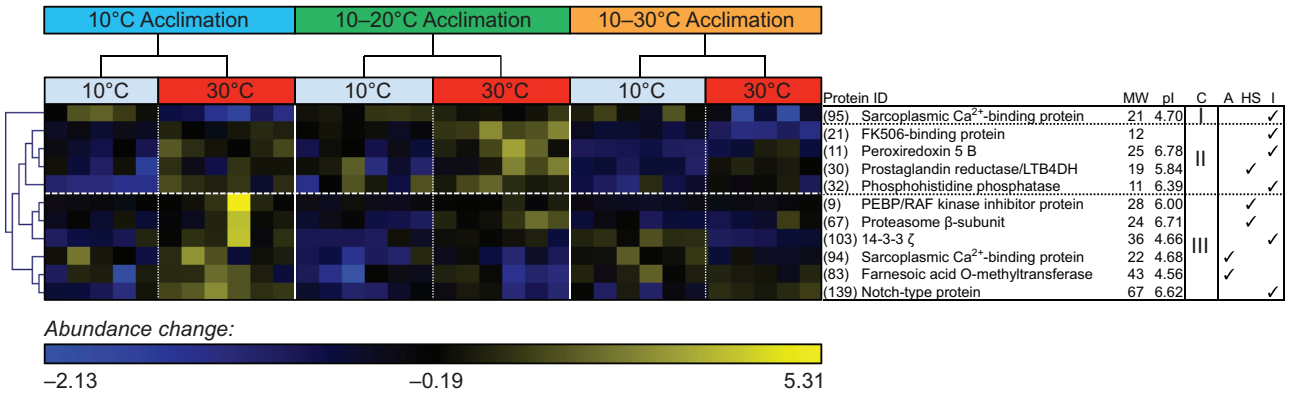


| Protein ID | MW | pI | C | A | HS | I |
|---|---|---|---|---|---|---|
| (95) Sarcoplasmic $Ca^{2+}$-binding protein | 21 | 4.70 | I | | | ✓ |
| (21) FK506-binding protein | 12 | | | | | ✓ |
| (11) Peroxiredoxin 5 B | 25 | 6.78 | II | | | ✓ |
| (30) Prostaglandin reductase/LTB4DH | 19 | 5.84 | | | ✓ | |
| (32) Phosphohistidine phosphatase | 11 | 6.39 | | | | ✓ |
| (9) PEBP/RAF kinase inhibitor protein | 28 | 6.00 | | | ✓ | |
| (67) Proteasome β-subunit | 24 | 6.71 | | | ✓ | |
| (103) 14-3-3 ζ | 36 | 4.66 | III | | | ✓ |
| (94) Sarcoplasmic $Ca^{2+}$-binding protein | 22 | 4.68 | | ✓ | | |
| (83) Farnesoic acid O-methyltransferase | 43 | 4.56 | | ✓ | | |
| (139) Notch-type protein | 67 | 6.62 | | | | ✓ |

**Fig. 9. Hierarchical clustering of changes in abundance of signaling proteins.** Pearson's correlation, in response to acclimation to daily temperature fluctuations and subsequent control (10°C) and heat shock (30°C) exposures from claw muscle tissue of the porcelain crab *Petrolisthes cinctipes*. For additional details, see Fig. 3.

The Journal of Experimental Biology (2015) doi:10.1242/jeb.112250

Although the exact function of SCPs is currently unknown (White et al., 2011), they are more highly expressed in fast twitch than slow tonic muscle tissue and serve as intracellular $Ca^{2+}$ buffers during contraction, similar to the function of parvalbumin. During the resting state, parvalbumin binds mostly $Mg^{2+}$, but during contraction it slowly releases $Mg^{2+}$ to take up $Ca^{2+}$. Tropomyosin blocks actin binding to myosin until troponin C takes up $Ca^{2+}$ (Clapham, 2007). Thus parvalbumin, and presumably SCP, limits competition with troponin C during contraction through slow $Ca^{2+}$ uptake, which increases efficiency of the actomyosin contractile apparatus (White et al., 2011; Berchtold et al., 2000; Wang and Metzger, 2008). Thus, it is possible that an increase in SCP leads to a sequestering of more $Ca^{2+}$ and therefore a change in the interaction between actin and myosin. Regulation of cytosolic $Mg^{2+}$ and $Ca^{2+}$ could also be important mechanisms for dealing with temperature-related environmental stress, because a change in $Mg^{2+}$ concentration is associated with cold shock in *P. clarkii* (White et al., 2011).

FK506-binding protein (FKBP) is a prolyl isomerase characterized by the binding of the immune suppressant FK506; it stabilizes the closed state of two calcium channels, ryanodine and $IP_3$ receptor (MacMillan, 2013). Its abundance increased, which suggests that muscle contraction is inhibited, with heat shock following acclimation to 10°C and 10–20°C.

### Sesquiterpenoid metabolism

Farnesoic acid *O*-methyltransferase (FaMeT) catalyzes the conversion from farnesoic acid to methyl farnesoate, a sesquiterpenoid that is involved in crustacean morphogenesis, reproduction and molting (Kuballa et al., 2011; Nagaraju, 2011). Transcripts for FaMeT have been detected in multiple crustacean tissues, including muscle (Nagaraju, 2011; Ruddell et al., 2003). The abundance of FaMeT increased with heat shock following acclimation to 10°C, decreased in response following 10–20°C, and increased again following 10–30°C (Fig. 9). Gill tissue showed changes in two FaMeT isoforms in response to pH and emersion stress (our unpublished data). Both, temperature and salinity affected testicular development in a MF-dependent fashion in *Carcinus maenas* (Nagaraju and Borst, 2008). Together, these results suggest an important role for FaMeT in the response of crustaceans to acute environmental stress.

### Inflammation

We identified five proteins of diverse functions that may be suppressing inflammation (Figs 9 and 10): RAF kinase inhibitor protein or (RKIP; also known as phosphatidylethanolamine-binding protein or PEBP) (Granovsky and Rosner, 2008), NADP-dependent leukotriene $B_4$ hydroxydehydrogenase ($LTB_4DH$) also known as prostaglandin reductase, a protein directly involved in the inactivation of the inflammatory mediator leukotriene $B_4$ ($LTB_4$), phosphohistidine phosphatase (PHP)-like janus protein, 14-3-3ζ and FKBP (see above). The four proteins possibly inhibiting inflammation fall into two clusters that show increasing abundances with heat shock following acclimation to 10–20°C (II: PGR and PHP) and 10°C (III: RKIP and 14-3-3). We hypothesize that heat shock suppresses inflammation after acclimation to 10°C and 10–20°C but not 10–30°C.

RKIP possibly represents a central node in a hypothetical network of signaling pathways that regulate inflammation (Fig. 10). RKIP inhibits the MEK-ERK1/2 MAP kinase module (Yeung et al., 2000; Yeung et al., 1999) and thereby the phosphorylation of phospholipase $A_2$, directly inhibiting the synthesis of pro-inflammatory prostanoids from arachidonic acid, including prostaglandin $E_2$ (PGE), via cyclooxygenase (COX) and leukotrienes, such as leukotriene $B_4$ ($LTB_4$) via lipooxygenase (LOX). Further downstream, prostaglandin reductase (PGR), which also functions as $LTB_4DH$, catabolizes PGE and $LTB_4$ into inactive metabolites, thereby suppressing an immune reaction and hemocyte recruitment (Marks et al., 2009; Tai, 2011). In addition to being

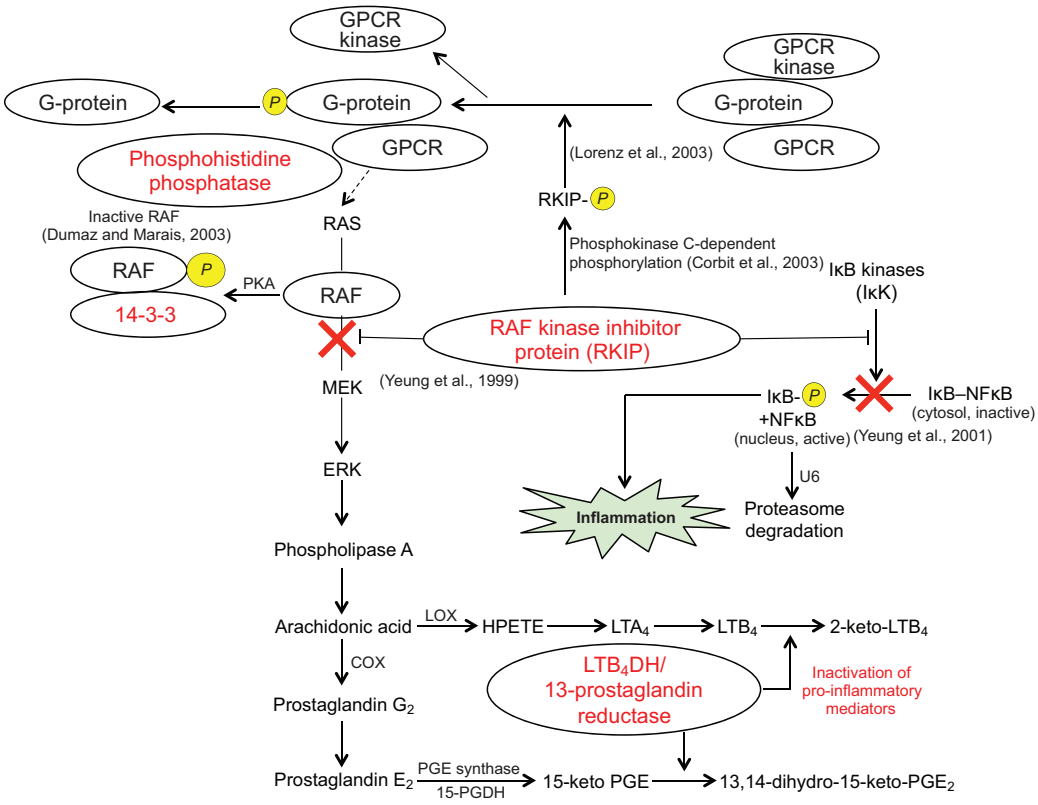


**Fig. 10. A schematic showing hypothetical pathways and cellular processes affected by changes in abundance of several signaling proteins that might inhibit an innate immune response.** Putative protein phosphorylation is indicated with yellow circles. Red text indicates signaling proteins; red crosses represent immune response. For details, see text. COX, cyclooxygenase; ERK, extracellular signal-regulated kinase; GPCR, G-protein coupled receptor; HPETE, arachidonic acid 5-hydroperoxide; IκB, inhibitor of kappa B; LOX, lipooxygenase; $LTA_4$, leukotriene $A_4$; $LTB_4$, leukotriene $B_4$; $LTB_4DH$, leukotriene $B_4$ hydroxydehydrogenase; MEK, mitogen-activated protein kinase kinase; NFκB, nuclear factor kappa B; PGDH, prostaglandin dehydrogenase; PGE, prostaglandin E; PKA, protein kinase A; RAF, rapidly accelerated fibrosarcoma.

The Journal of Experimental Biology (2015) doi:10.1242/jeb.112250

inhibited by RKIP, RAF kinase, as part of the ERK1/2 MAP kinase module, can be inhibited if it gets phosphorylated by protein kinase A (PKA) and subsequently sequestered from the membrane by 14-3-3 (Dumaz and Marais, 2003). RKIP also interferes with the activation of the pro-inflammatory transcription factor nuclear kappa B (NFκB) by inhibiting the phosphorylation of the inhibitor protein IκB through IκB kinase, which, in turn, inhibits the disassociation of NFκB–IκB to an active form of NFκB (Yeung et al., 2001). Finally, phosphorylated RKIP binds to G-protein-coupled receptor kinase (GPCR kinase or GRK), leading to the dissociation of a G-protein–GPCR complex and prolonged G-protein signaling (Keller et al., 2004; Lorenz et al., 2003). Interestingly, it is a GPCR that activates the ERK1/2 module. Furthermore, it is possible that a β-subunit of the G-protein is a substrate of phosphohistidine phosphatase (PHP) (Lorenz et al., 2003).

Notch is a transmembrane receptor protein that is activated by ligands from other cells during development, triggering the proteolytic cleavage of the intracellular domain of notch, which activates gene expression by the NFκB-like transcription factor CSL (Marks et al., 2009). Also, there is evidence for a synergistic interaction between notch and NFκB (Barbarulo et al., 2011). Furthermore, notch seems to modulate cellular metabolism, specifically glucose uptake and glycolysis (Ciofani and Zúñiga-Pflücker, 2005; Graziani et al., 2008; Landor et al., 2011), and thus might be involved in regulating some of the changes in abundance of glycolytic enzymes with heat shock following acclimation to 10°C.

### Conclusion

PCAs based on the significantly changing proteins showed that the response to heat shock is greater following acclimation to 10°C and 10–30°C in comparison to 10–20°C (Fig. 2). Thus, the 10–30°C acclimation regime was severe enough that porcelain crabs did not acclimate to a daily occurrence of a 30°C heat shock. The fact that the response to heat shock following acclimation to 10–20°C was limited, suggests that the proteomic changes that occurred during acclimation increased resistance to a subsequent 30°C heat shock. However, there are few changes accompanying the 10–20°C acclimation regime per se. Increasing levels of actin fragments and the actin-binding proteins cofilin, gelsolin and actinin with heat shock following acclimation to 10–20°C suggest that organisms are instead primed to deal with heat shock by changing actin filament structure and possible dynamics while changing other cellular processes only to a limited extent. In this context, it is worth noting that we did not detect any molecular chaperones in any of the treatments, with the exception of FKBP, most likely because they are less abundant than the proteins we detected (Carberry et al., 2014).

Heat shock following acclimation to 10°C is presumably the most stressful of our treatments, as indicated by PCA (Fig. 2C). Heat shock caused a strong increase in ATP-buffering (Fig. 3, cluster III), glycolysis (one GAPDH), actomyosin restructuring (two paramyosin and MHC isoforms), a number of ABP and signaling proteins that might suppress an immune response. Heat shock after acclimation to 10–30°C was similarly stressful, based on our PCAs (Fig. 2A,B). Acclimation to daily 10–30°C (measured at 10°C) increased ATP-buffering, metabolic (enolase, phosphoglycerate kinase and ATP synthase), respiratory (hemocyanin) and filament (MHC and actin) proteins. A subsequent 30°C heat shock increased ATP-buffering, different metabolic (TPI, GAPDH, enolase and PDH), one respiratory (hemocyanin) and several filament (MHC and actin) proteins as well as actin-binding proteins that stabilize actin filaments (filamin, actinin and tropomyosin).

Thus, temperature fluctuations always require ATP buffering and greater fluctuations require modifications of glycolytic proteins and ATP synthase, as well as an increase in hemocyanins. Chronic temperature fluctuations require modifications in thick and thin filaments. Most importantly, moderate temperature fluctuations are characterized by proteins that depolymerize and sever actin filaments, possibly to restructure actomyosin fibers to modify ATP-turnover rates, whereas extreme temperature fluctuations increase the proteins that stabilize actin filaments. It is possible that both changes cause actomyosin fibers to modify their functional properties. Finally, acute heat shock inhibits inflammation, possibly making crustaceans more susceptible to pathogens.

The proteome of claw muscle adjusted to temperature fluctuations by modifying proteins involved in ATP production, oxygen transport, the structure and dynamics of the actomyosin complex and inflammation. Acute heat shock is always the dominant driver of these changes. Acclimation to 10°C caused the greatest proteomic changes, acclimation to 10–20°C required few additional proteomic modifications and acclimation to 10–30°C required intermediate proteomic changes in response to a subsequent acute 30°C heat shock. The daily occurrence of an acute 30°C heat shock is thus above the threshold at which *P. cinctipes* is able to fully acclimate. Our results suggest that whereas intertidal crustaceans are already experiencing great temperature fluctuations, which are preparing the animals for a subsequent greater heat shock, more extreme fluctuations will be physiologically costly because of the daily and broad modifications of the proteome associated with such shifts in temperature ranges.

## MATERIALS AND METHODS

### Animal collection, maintenance and experimental design

Adult *Petrolisthes cinctipes* (Randall, 1839) were collected from the intertidal zone of Fort Ross, CA, USA (38°30′51″ N, 123°14′34″ W) in October 2008. The crabs were transported to the Romberg Tiburon Center for Environmental Studies (San Francisco State University, Tiburon, CA, USA), where they were maintained in a common garden acclimation under constant immersion at 10°C for 30 days. Following the common garden, crabs were randomly placed into three treatment groups. Over 30 days, these groups experienced acclimation at either 10°C (‘constant’) or daily heat ramps from 10–20°C (‘moderate’) or 10–30°C (‘extreme’). All thermal acclimations had temperature precision of at least ±0.5°C. In the two groups that experienced heat ramping, temperature was gradually increased over a 5 h period to the respective peak temperature, and then cooled to 10°C over 1 h. After these temperature acclimations, crabs from each treatment were randomly placed in either a constant 10°C immersion or given a ramp-up to 30°C heat shock over 5 h. All individuals were given a 1 h recovery period at 10°C before being flash frozen in liquid nitrogen and stored at −80°C. Four claw segments (dactyl, propodus, carpus, and merus) were dissected and transported to the Environmental Proteomics Laboratory (Cal Poly, San Luis Obispo, CA, USA) on dry ice for proteomic analysis.

The preparation of the muscle tissue samples and the exploratory statistical analyses following published protocols and procedures (Fields et al., 2012b; Serafini et al., 2011; Tomanek and Zuzow, 2010; Tomanek et al., 2012; Tomanek et al., 2011) are described below. We analyzed tissues from $N$=5–6 animals per treatment (Figs 3–9). There was no mortality recorded during acclimation and following the acute heat shock treatment.

### Homogenization

Claw tissue was lysed in ground glass homogenizers in a 1:4 ratio of homogenization buffer [7 mol $l^{-1}$ urea, 2 mol $l^{-1}$ thiourea, 1% ASB (amidosulfobetaine)-14, 40 mmol $l^{-1}$ Tris-base, 40 mmol $l^{-1}$ dithiothreitol and 0.5% immobilized pH 4–7 gradient (IPG) buffer (GE Healthcare, Piscataway, NJ, USA)], solubilized at 20°C for 1 h, and then centrifuged at 16,100 ***g*** for 30 min at 20°C. Proteins were precipitated from the supernatant using a 1:4 ratio of ice-cold 10% trichloroacetic acid in acetone with an

overnight incubation at −20°C. The samples were centrifuged at 18,000 ***g*** for 15 min at 4°C, after which the supernatant was discarded and the protein pellet washed with ice-cold acetone. Samples were again centrifuged according to the previous parameters and the supernatant was discarded. After briefly drying in air, the protein pellets were re-suspended in rehydration buffer [7 mol $l^{-1}$ urea, 2 mol $l^{-1}$ thiourea, 2% CHAPS (cholamidopropyldimethylammonio-propanesulfonic acid), 2% NP (nonyl phenoxylpolyethoxylethanol)-40, 0.002% Bromophenol Blue, 0.5% IPG (4-7) buffer and 100 mmol $l^{-1}$ dithioerythritol] and solubilized at 20°C for 1 h. To determine the protein concentration in each sample, a concentration assay was performed using the 2-D QuantKit (GE Healthcare) according to the manufacturer's instructions.

### Two-dimensional gel electrophoresis

For first dimension electrophoresis, proteins were separated according to their isoelectric points (pI), using IPG gel strips (pH 4–7, 11 cm; GE Healthcare). Protein samples were diluted to a concentration of 2 µg $µl^{-1}$ in rehydration buffer and 200 µl (400 µg) was loaded onto each IPG gel strip in one well of an isoelectric focusing cell (Bio-Rad, Hercules, CA, USA). Protein solution was absorbed into each IPG gel strip over 5 h of passive rehydration followed by 12 h of active rehydration at 50 V. Separation and focusing of proteins was performed by running gel strips at 500 V for 1 h, 1000 V for 1 h and then 8000 V for 2.5 h (maximum current 50 µA; all voltage changes occurred in rapid mode). After isoelectric focusing, gel strips were frozen at −80°C. After freezing for at least 1 h, gel strips were prepared for second dimension SDS-PAGE by incubating them in equilibration buffer (6 mol $l^{-1}$ urea, 375 mmol $l^{-1}$ Tris base, 30% glycerol, 2% SDS, 0.002% Bromophenol Blue) at 20°C for two 15 min intervals, first with 65 mol $l^{-1}$ dithiothreitol and then with 135 mol $l^{-1}$ iodoacetamide. Gel strips were then placed over 11.8% polyacrylamide gels and run (Criterion Dodeca; Bio-Rad) for 55 min at 200 V. Following electrophoresis, gels were stained using colloidal Coomassie Blue (G-250) overnight and then destained through repeated washing with milliQ water over 48 h. Gels were then scanned with an Epson 1280 transparency scanner (Epson, Long Beach, CA, USA).

### Gel image analysis

Digitized 2D gel images were analyzed using Delta 2D (version 3.6; Decodon, Greifswald, Germany) (Berth et al., 2007). To detect protein spots, gels from all treatments were multiplexed into a single fused image. The spot boundaries detected on the fused image were transferred back to the individual gels, establishing protein spot parameters for each gel. Following background subtraction, the relative spot volume of each protein was quantified by normalization against the total spot volume of all proteins in the gel image.

### Mass spectrometry

Gel plugs were prepared for analysis using mass spectrometry (MS) according to previously published methods (Fields et al., 2012; Tomanek and Zuzow, 2010). Briefly, peptide mass fingerprints (PMFs) were obtained using a matrix-assisted laser desorption/ionization tandem time-of-flight (MALDI-ToF-ToF) mass spectrometer (UltraFlex II; Bruker Daltonics, Inc., Billerica, MA, USA). To obtain *b*- and *y*-ion parameters, at least six peptides were selected for tandem MS. Spectral analysis of peptides followed previously published methods (Fields et al., 2012; Tomanek and Zuzow, 2010). FlexAnalysis (version 3.0; Bruker Daltonic, Inc.) was used to detect peptide peaks, using a signal-to-noise ratio of 6 for MS and 1.5 for MS/MS. Internal mass calibration was performed using porcine trypsin. Proteins were identified using Mascot (version 2.2; Matrix Science, Inc., Boston, MA). PMFs and tandem mass spectra were combined and searched against the Porcelain Crab Array Database (PCAD), an EST library for *P. cinctipes* that contains 19,000 unique sequences (Tagmount et al., 2010). Spectra that could not be identified with PCAD were searched against an EST library for the boreal spider crab *Hyas araneus* (Harms et al., 2013). One missed cleavage was allowed during searches. For the MS/MS analysis, the precursor-ion mass tolerance was set at 0.6 Da (default Mascot value). Search results were deemed significant ($P \leq 0.05$) if their molecular weight search (MOWSE) score was 42 or higher for PCAD and 34 or higher for the *H. araneus* EST. For results with a significant MOWSE score, only positive identifications that included two matched peptide sequences were accepted.

### Exploratory statistical analysis

We compared protein abundances between treatment groups via average linking of individual gels (Delta 2D) using a Pearson correlation metric. We performed a two-way ANOVA ($P \leq 0.02$) comparing thermal acclimation versus acute heat shock effects and grouped significantly changing proteins into hierarchical clusters. To better understand the importance of particular proteins in characterizing the proteomic response to different temperature treatments, we used PCA (Delta 2D) based on proteins whose expression profiles significantly changed, regardless of whether they were identified with MS. Of the proteins that were identified with MS, we assigned component loading values which are quantifications of a protein's contribution to sample separation along a given component.

#### Acknowledgements

We thank Claudia Tomas-Miranda and Paula Robinson for invaluable assistance during the experiment and Dr Christina Vasquez for helpful editorial comments.

#### Competing interests

The authors declare no competing or financial interests.

#### Author contributions

M.A.G., J.H.S. and L.T. designed the experiment and analysis of the samples. M.A.G. and L.T. analyzed the data and wrote the manuscript.

#### Funding

The study was supported by a grant from the Council of Ocean Affairs, Science and Technology (COAST) to M.A.G. and National Science Foundation grants (MCB-1041225 to J.H.S. and EF-1041227 to L.T.).

#### Supplementary material

Supplementary material available online at
http://jeb.biologists.org/lookup/suppl/doi:10.1242/jeb.112250/-/DC1

#### References

**Abe, H., Hirai, S. and Okada, S.** (2007). Metabolic responses and arginine kinase expression under hypoxic stress of the kuruma prawn *Marsupenaeus japonicus*. *Comp. Biochem. Physiol.* **146A**, 40-46.

**Ahearn, G. A., Mandal, P. K. and Mandal, A.** (2004). Calcium regulation in crustaceans during the molt cycle: a review and update. *Comp. Biochem. Physiol.* **137A**, 247-257.

**Barbarulo, A., Grazioli, P., Campese, A. F., Bellavia, D., Di Mario, G., Pelullo, M., Ciuffetta, A., Colantoni, S., Vacca, A., Frati, L. et al.** (2011). Notch3 and canonical NF-kappaB signaling pathways cooperatively regulate Foxp3 transcription. *J. Immunol.* **186**, 6199-6206.

**Berchtold, M. W., Brinkmeier, H. and Müntener, M.** (2000). Calcium ion in skeletal muscle: its crucial role for muscle function, plasticity, and disease. *Physiol. Rev.* **80**, 1215-1265.

**Bjelde, B. E. and Todgham, A. E.** (2013). Thermal physiology of the fingered limpet *Lottia digitalis* under emersion and immersion. *J. Exp. Biol.* **216**, 2858-2869.

**Burmester, T.** (2001). Molecular evolution of the arthropod hemocyanin superfamily. *Mol. Biol. Evol.* **18**, 184-195.

**Carberry, S., Zweyer, M., Swandulla, D. and Ohlendieck, K.** (2014). Comparative proteomic analysis of the contractile-protein-depleted fraction from normal versus dystrophic skeletal muscle. *Anal. Biochem.* **446**, 108-115.

**Cayenne, A. P., Gabert, B. and Stillman, J. H.** (2011). Identification of proteins interacting with lactate dehydrogenase in claw muscle of the porcelain crab *Petrolisthes cinctipes*. *Comp. Biochem. Physiol.* **6D**, 393-398.

**Chen, X. and Stillman, J. H.** (2012). Multigenerational analysis of temperature and salinity variability affects on metabolic rate, generation time and actue thermal and salinity tolerance in *Daphnia pulex*. *J. Therm. Biol.* **37**, 185-194.

**Chongsatja, P. O., Bourchookarn, A., Lo, C. F., Thongboonkerd, V. and Krittanai, C.** (2007). Proteomic analysis of differentially expressed proteins in *Penaeus vannamei* hemocytes upon Taura syndrome virus infection. *Proteomics* **7**, 3592-3601.

**Ciofani, M. and Zúñiga-Pflücker, J. C.** (2005). Notch promotes survival of pre-T cells at the beta-selection checkpoint by regulating cellular metabolism. *Nat. Immunol.* **6**, 881-888.

**Clapham, D. E.** (2007). Calcium signaling. *Cell* **131**, 1047-1058.

**Clark, K. A., McElhinny, A. S., Beckerle, M. C. and Gregorio, C. C.** (2002). Striated muscle cytoarchitecture: an intricate web of form and function. *Annu. Rev. Cell Dev. Biol.* **18**, 637-706.

**Dalle-Donne, I., Rossi, R., Colombo, G., Giustarini, D. and Milzani, A.** (2009). Protein S-glutathionylation: a regulatory device from bacteria to humans. *Trends Biochem. Sci.* **34**, 85-96.

**Decker, H. and Jaenicke, E.** (2004). Recent findings on phenoloxidase activity and antimicrobial activity of hemocyanins. *Dev. Comp. Immunol.* **28**, 673-687.
**Destoumieux-Garzón, D., Saulnier, D., Garnier, J., Jouffrey, C., Bulet, P. and Bachère, E.** (2001). Crustacean immunity. Antifungal peptides are generated from the C terminus of shrimp hemocyanin in response to microbial challenge. *J. Biol. Chem.* **276**, 47070-47077.
**Dilly, G. F., Young, C. R., Lane, W. S., Pangilinan, J. and Girguis, P. R.** (2012). Exploring the limit of metazoan thermal tolerance via comparative proteomics: thermally induced changes in protein abundance by two hydrothermal vent polychaetes. *Proc. Biol. Sci.* **279**, 3347-3356.
**Dumaz, N. and Marais, R.** (2003). Protein kinase A blocks Raf-1 activity by stimulating 14-3-3 binding and blocking Raf-1 interaction with Ras. *J. Biol. Chem.* **278**, 29819-29823.
**Dzeja, P. P. and Terzic, A.** (2003). Phosphotransfer networks and cellular energetics. *J. Exp. Biol.* **206**, 2039-2047.
**Ellington, W. R.** (2001). Evolution and physiological roles of phosphagen systems. *Annu. Rev. Physiol.* **63**, 289-325.
**Fields, P. A., Cox, K. M. and Karch, K. R.** (2012a). Latitudinal variation in protein expression after heat stress in the salt marsh mussel *Geukensia demissa*. *Integr. Comp. Biol.* **52**, 636-647.
**Fields, P. A., Zuzow, M. J. and Tomanek, L.** (2012b). Comparative proteomics of blue mussel (*Mytilus*) congeners to temperature acclimation. *J. Exp. Biol.* **215**, 1106-1116.
**Fischer, E. H.** (2013). Cellular regulation by protein phosphorylation. *Biochem. Biophys. Res. Commun.* **430**, 865-867.
**Fratelli, M., Demol, H., Puype, M., Casagrande, S., Villa, P., Eberini, I., Vandekerckhove, J., Gianazza, E. and Ghezzi, P.** (2003). Identification of proteins undergoing glutathionylation in oxidatively stressed hepatocytes and hepatoma cells. *Proteomics* **3**, 1154-1161.
**Gao, Y., Gillen, C. M. and Wheatly, M. G.** (2006). Molecular characterization of the sarcoplasmic calcium-binding protein (SCP) from crayfish *Procambarus clarkii*. *Comp. Biochem. Physiol.* **144B**, 478-487.
**Götz, R., Schlüter, E., Shoham, G. and Zimmermann, F. K.** (1999). A potential role of the cytoskeleton of *Saccharomyces cerevisiae* in a functional organization of glycolytic enzymes. *Yeast* **15**, 1619-1629.
**Granovsky, A. E. and Rosner, M. R.** (2008). Raf kinase inhibitory protein: a signal transduction modulator and metastasis suppressor. *Cell Res.* **18**, 452-457.
**Graziani, I., Eliasz, S., De Marco, M. A., Chen, Y., Pass, H. I., De May, R. M., Strack, P. R., Miele, L. and Bocchetta, M.** (2008). Opposite effects of Notch-1 and Notch-2 on mesothelioma cell survival under hypoxia are exerted through the Akt pathway. *Cancer Res.* **68**, 9678-9685.
**Griffiths, J. R.** (1981). A fresh look at glycogenolysis in skeletal muscle. *Biosci. Rep.* **1**, 595-610.
**Havanapan, P. O., Kanlaya, R., Bourchookarn, A., Krittanai, C. and Thongboonkerd, V.** (2009). C-terminal hemocyanin from hemocytes of *Penaeus vannamei* interacts with ERK1/2 and undergoes serine phosphorylation. *J. Proteome Res.* **8**, 2476-2483.
**Hermann, A. and Cox, J. A.** (1995). Sarcoplasmic calcium-binding protein. *Comp. Biochem. Physiol.* **111B**, 337-345.
**Hochachka, P. W.** (2003). Intracellular convection, homeostasis and metabolic regulation. *J. Exp. Biol.* **206**, 2001-2009.
**Hochachka, P. W. and Somero, G. N.** (2002). *Biochemical Adaptation: Mechanism and Process in Physiological Evolution*. Oxford: Oxford University Press.
**Hooper, S. L., Hobbs, K. H. and Thuma, J. B.** (2008). Invertebrate muscles: thin and thick filament structure; molecular basis of contraction and its regulation, catch and asynchronous muscle. *Prog. Neurobiol.* **86**, 72-127.
**Keller, E. T., Fu, Z. and Brennan, M.** (2004). The role of Raf kinase inhibitor protein (RKIP) in health and disease. *Biochem. Pharmacol.* **68**, 1049-1053.
**Kim, B. K., Kim, K. S., Oh, C.-W., Mykles, D. L., Lee, S. G., Kim, H. J. and Kim, H.-W.** (2009). Twelve actin-encoding cDNAs from the American lobster, *Homarus americanus*: cloning and tissue expression of eight skeletal muscle, one heart, and three cytoplasmic isoforms. *Comp. Biochem. Physiol.* **153B**, 178-184.
**Kothakota, S., Azuma, T., Reinhard, C., Klippel, A., Tang, J., Chu, K., McGarry, T. J., Kirschner, M. W., Koths, K., Kwiatkowski, D. J. et al.** (1997). Caspase-3-generated fragment of gelsolin: effector of morphological change in apoptosis. *Science* **278**, 294-298.
**Kuballa, A. V., Holton, T. A., Paterson, B. and Elizur, A.** (2011). Moult cycle specific differential gene expression profiling of the crab *Portunus pelagicus*. *BMC Genomics* **12**, 147.
**Landor, S. K., Mutvei, A. P., Mamaeva, V., Jin, S., Busk, M., Borra, R., Grönroos, T. J., Kronqvist, P., Lendahl, U. and Sahlgren, C. M.** (2011). Hypo- and hyperactivated Notch signaling induce a glycolytic switch through distinct mechanisms. *Proc. Natl. Acad. Sci. USA* **108**, 18814-18819.
**Lee, S. H. and Dominguez, R.** (2010). Regulation of actin cytoskeleton dynamics in cells. *Mol. Cells* **29**, 311-325.
**Lee, S. Y., Lee, B. L. and Söderhäll, K.** (2003). Processing of an antibacterial peptide from hemocyanin of the freshwater crayfish *Pacifastacus leniusculus*. *J. Biol. Chem.* **278**, 7927-7933.
**Levitsky, D. I., Pivovarova, A. V., Mikhailova, V. V. and Nikolaeva, O. P.** (2008). Thermal unfolding and aggregation of actin. *FEBS J.* **275**, 4280-4295.
**Lorenz, K., Lohse, M. J. and Quitterer, U.** (2003). Protein kinase C switches the Raf kinase inhibitor from Raf-1 to GRK-2. *Nature* **426**, 574-579.
**Macias, M. T. and Sastre, L.** (1990). Molecular cloning and expression of four actin isoforms during *Artemia* development. *Nucleic Acids Res.* **18**, 5219-5225.
**MacMillan, D.** (2013). FK506 binding proteins: cellular regulators of intracellular $Ca^{2+}$ signalling. *Eur. J. Pharmacol.* **700**, 181-193.
**Marks, F., Klingmüller, U. and Müller-Decker, K.** (2009). *Cellular Signal Processing: an Introduction to the Molecular Mechanisms of Signal Transduction*. New York, NY: Garland Science, Taylor and Francis Group.
**Medler, S., Lilley, T. and Mykles, D. L.** (2004). Fiber polymorphism in skeletal muscles of the American lobster, *Homarus americanus*: continuum between slow-twitch (S1) and slow-tonic (S2) fibers. *J. Exp. Biol.* **207**, 2755-2767.
**Murakami, K., Stewart, M., Nozawa, K., Tomii, K., Kudou, N., Igarashi, N., Shirakihara, Y., Wakatsuki, S., Yasunaga, T. and Wakabayashi, T.** (2008). Structural basis for tropomyosin overlap in thin (actin) filaments and the generation of a molecular swivel by troponin-T. *Proc. Natl. Acad. Sci. USA* **105**, 7200-7205.
**Myers, C. D., Goh, P. Y., Allen, T. S., Bucher, E. A. and Bogaert, T.** (1996). Developmental genetic analysis of troponin T mutations in striated and nonstriated muscle cells of *Caenorhabditis elegans*. *J. Cell Biol.* **132**, 1061-1077.
**Mykles, D. L.** (1997). Crustacean muscle plasticity: molecular mechanisms determining mass and contractile properties. *Comp. Biochem. Physiol.* **117B**, 367-378.
**Mykles, D. L. and Haire, M. F.** (1991). Sodium dodecyl sulfate and heat induce two distinct forms of lobster muscle multicatalytic proteinase: the heat-activated form degrades myofibrillar proteins. *Arch. Biochem. Biophys.* **288**, 543-551.
**Nagaraju, G. P.** (2011). Reproductive regulators in decapod crustaceans: an overview. *J. Exp. Biol.* **214**, 3-16.
**Nagaraju, G. P. and Borst, D. W.** (2008). Methyl farnesoate couples environmental changes to testicular development in the crab *Carcinus maenas*. *J. Exp. Biol.* **211**, 2773-2778.
**Ortega, M. A., Macias, M. T., Martinez, J. L., Palmero, I. and Sastre, L.** (1992). Expression of actin isoforms in Artemia. *Symp. Soc. Exp. Biol.* **46**, 131-137.
**Podrabsky, J. E. and Somero, G. N.** (2004). Changes in gene expression associated with acclimation to constant temperatures and fluctuating daily temperatures in an annual killifish *Austrofundulus limnaeus*. *J. Exp. Biol.* **207**, 2237-2254.
**Reddy, S., Jones, A. D., Cross, C. E., Wong, P. S. and Van Der Vliet, A.** (2000). Inactivation of creatine kinase by S-glutathionylation of the active-site cysteine residue. *Biochem. J.* **347**, 821-827.
**Rock, J., Magnay, J. L., Beech, S., El Haj, A. J., Goldspink, G., Lunt, D. H. and Whiteley, N. M.** (2009). Linking functional molecular variation with environmental gradients: myosin gene diversity in a crustacean broadly distributed across variable thermal environments. *Gene* **437**, 60-70.
**Ruddell, C. J., Wainwright, G., Geffen, A., White, M. R., Webster, S. G. and Rees, H. H.** (2003). Cloning, characterization, and developmental expression of a putative farnesoic acid O-methyl transferase in the female edible crab *Cancer pagurus*. *Biol. Bull.* **205**, 308-318.
**Serafini, L., Hann, J. B., Kültz, D. and Tomanek, L.** (2011). The proteomic response of sea squirts (genus *Ciona*) to acute heat stress: a global perspective on the thermal stability of proteins. *Comp. Biochem. Physiol.* **6D**, 322-334.
**Somero, G. N.** (2012). The physiology of global change: linking patterns to mechanisms. *Ann. Rev. Mar. Sci.* **4**, 39-61.
**Squire, J. M.** (2009). Muscle myosin filaments: cores, crowns, and couplings. *Biophys. Rev.* **1**, 149-160.
**Stillman, J. H.** (2003). Acclimation capacity underlies susceptibility to climate change. *Science* **301**, 65.
**Stillman, J. H. and Somero, G. N.** (2000). A comparative analysis of the upper thermal tolerance limits of eastern Pacific porcelain crabs, genus *Petrolisthes*: influences of latitude, vertical zonation, acclimation, and phylogeny. *Physiol. Biochem. Zool.* **73**, 200-208.
**Suarez-Herta, N., Lecocq, R., Mosselmans, R., Galand, P., Dumont, J. E. and Robaye, B.** (2000). Myosin heavy chain degradation during apoptosis in endothelial cells. *Cell Prolif.* **33**, 101-114.
**Tagmount, A., Wang, M., Lindquist, E., Tanaka, Y., Teranishi, K. S., Sunagawa, S., Wong, M. and Stillman, J. H.** (2010). The porcelain crab transcriptome and PCAD, the porcelain crab microarray and sequence database. *PLoS ONE* **5**, e9327.
**Tai, H. H.** (2011). Prostaglandin catabolic enzymes as tumor suppressors. *Cancer Metastasis Rev.* **30**, 409-417.
**Teranishi, K. S. and Stillman, J. H.** (2007). A cDNA microarray analysis of the response to heat stress in hepatopancreas tissue of the porcelain crab *Petrolisthes cinctipes*. *Comp. Biochem, Physiol.* **2D**, 53-62.
**Tohtong, R., Yamashita, H., Graham, M., Haeberle, J., Simcox, A. and Maughan, D.** (1995). Impairment of muscle function caused by mutations of phosphorylation sites in myosin regulatory light chain. *Nature* **374**, 650-653.
**Tomanek, L.** (2010). Variation in the heat shock response and its implication for predicting the effect of global climate change on species' biogeographical distribution ranges and metabolic costs. *J. Exp. Biol.* **213**, 971-979.
**Tomanek, L.** (2011). Environmental proteomics: changes in the proteome of marine organisms in response to environmental stress, pollutants, infection, symbiosis, and development. *Ann. Rev. Mar. Sci.* **3**, 373-399.
**Tomanek, L.** (2014). Proteomics to study adaptations in marine organisms to environmental stress. *J. Proteomics* **105**, 92-106.
**Tomanek, L. and Somero, G. N.** (1999). Evolutionary and acclimation-induced variation in the heat-shock responses of congeneric marine snails (genus *Tegula*) from different thermal habitats: implications for limits of thermotolerance and biogeography. *J. Exp. Biol.* **202**, 2925-2936.
**Tomanek, L. and Somero, G. N.** (2000). Time course and magnitude of synthesis of heat-shock proteins in congeneric marine snails (genus *Tegula*) from different tidal heights. *Physiol. Biochem. Zool.* **73**, 249-256.
**Tomanek, L. and Zuzow, M. J.** (2010). The proteomic response of the mussel congeners *Mytilus galloprovincialis* and *M. trossulus* to acute heat stress:

implications for thermal tolerance limits and metabolic costs of thermal stress. *J. Exp. Biol.* **213**, 3559-3574.

**Tomanek, L., Zuzow, M. J., Ivanina, A. V., Beniash, E. and Sokolova, I. M.** (2011). Proteomic response to elevated $P_{CO_2}$ level in eastern oysters, *Crassostrea virginica*: evidence for oxidative stress. *J. Exp. Biol.* **214**, 1836-1844.

**Tomanek, L., Zuzow, M. J., Hitt, L., Serafini, L. and Valenzuela, J. J.** (2012). Proteomics of hyposaline stress in blue mussel congeners (genus *Mytilus*): implications for biogeographic range limits in response to climate change. *J. Exp. Biol.* **215**, 3905-3916.

**Ubuka, T., Masuoka, N., Yoshida, S. and Ishino, K.** (1987). Determination of isoelectric point value of 3-mercaptopyruvate sulfurtransferase by isoelectric focusing using ribonuclease A-glutathione mixed disulfides as standards. *Anal. Biochem.* **167**, 284-289.

**Uda, K., Fujimoto, N., Akiyama, Y., Mizuta, K., Tanaka, K., Ellington, W. R. and Suzuki, T.** (2006). Evolution of the arginine kinase gene family. *Comp. Biochem. Physiol.* **1D**, 209-218.

**van der Flier, A. and Sonnenberg, A.** (2001). Structural and functional aspects of filamins. *Biochim. Biophys. Acta* **1538**, 99-117.

**VanBuren, P., Waller, G. S., Harris, D. E., Trybus, K. M., Warshaw, D. M. and Lowey, S.** (1994). The essential light chain is required for full force production by skeletal muscle myosin. *Proc. Natl. Acad. Sci. USA* **91**, 12403-12407.

**Varadaraj, K., Kumari, S. S. and Skinner, D. M.** (1996). Actin-encoding cDNAs and gene expression during the intermolt cycle of the Bermuda land crab *Gecarcinus lateralis*. *Gene* **171**, 177-184.

**Wang, W. and Metzger, J. M.** (2008). Parvalbumin isoforms for enhancing cardiac diastolic function. *Cell Biochem. Biophys.* **51**, 1-8.

**Wegner, A.** (1982). Kinetic analysis of actin assembly suggests that tropomyosin inhibits spontaneous fragmentation of actin filaments. *J. Mol. Biol.* **161**, 217-227.

**White, A. J., Northcutt, M. J., Rohrback, S. E., Carpenter, R. O., Niehaus-Sauter, M. M., Gao, Y., Wheatly, M. G. and Gillen, C. M.** (2011). Characterization of sarcoplasmic calcium binding protein (SCP) variants from freshwater crayfish *Procambarus clarkii*. *Comp. Biochem. Physiol.* **160B**, 8-14.

**Widdows, J.** (1976). Physiological adaptation of *Mytilus edulis* to cyclic temperatures. *J. Comp. Physiol.* **105**, 115-128.

**Wolosker, H., Panizzutti, R. and Engelender, S.** (1996). Inhibition of creatine kinase by S-nitrosoglutathione. *FEBS Lett.* **392**, 274-276.

**Yeung, K., Seitz, T., Li, S., Janosch, P., McFerran, B., Kaiser, C., Fee, F., Katsanakis, K. D., Rose, D. W., Mischak, H. et al.** (1999). Suppression of Raf-1 kinase activity and MAP kinase signalling by RKIP. *Nature* **401**, 173-177.

**Yeung, K., Janosch, P., McFerran, B., Rose, D. W., Mischak, H., Sedivy, J. M. and Kolch, W.** (2000). Mechanism of suppression of the Raf/MEK/extracellular signal-regulated kinase pathway by the raf kinase inhibitor protein. *Mol. Cell. Biol.* **20**, 3079-3085.

**Yeung, K. C., Rose, D. W., Dhillon, A. S., Yaros, D., Gustafsson, M., Chatterjee, D., McFerran, B., Wyche, J., Kolch, W. and Sedivy, J. M.** (2001). Raf kinase inhibitor protein interacts with NF-kappaB-inducing kinase and TAK1 and inhibits NF-kappaB activation. *Mol. Cell. Biol.* **21**, 7207-7217.

**Zhou, W., Capello, M., Fredolini, C., Piemonti, L., Liotta, L. A., Novelli, F. and Petricoin, E. F.** (2010). Mass spectrometry analysis of the post-translational modifications of alpha-enolase from pancreatic ductal adenocarcinoma cells. *J. Proteome Res.* **9**, 2929-2936.

**Table S1: Protein identification with estimated and predicted molecular mass (kDa), isoelectric point (pI), GenBank identifier, MASCOT score, number of peptides matched, sequence coverage, and putative functional category.**

| Spot ID | Protein ID | A | HS | I | Estimated MW | Estimated pI | Predicted MW | Predicted pI | GenBank ID | Mascot Score | Peptide Matches | Sequence Coverage | Functional Category |
|---|---|---|---|---|---|---|---|---|---|---|---|---|---|
| 3 | Paramyosin (long form) | | ✓ | | 69 | 6.40 | 103.02 | 5.46 | isotig00035 | 77 | 3 | 1% | Thick filament |
| 4 | Arginine kinase | | ✓ | | 35 | 5.93 | 39.96 | 6.05 | gi\|170186144 | 170 | 5 | 20% | Phosphotransfer |
| 5 | Arginine kinase | | | ✓ | 31 | 6.47 | 39.96 | 6.05 | gi\|170187671 | 391 | 8 | 42% | Phosphotransfer |
| 6 | Cardiac-like muscle actin | | ✓ | | 31 | 6.03 | 41.65 | 5.23 | gi\|170182268 | 167 | 3 | 14% | Thin filament |
| 7 | Arginine kinase | | | ✓ | 28 | 6.58 | 39.96 | 6.05 | gi\|170186144 | 294 | 7 | 29% | Phosphotransfer |
| 8 | Glyceraldehyde-3-phosphate dehydrogenase | | ✓ | | 28 | 6.24 | 18.66 | 5.58 | gi\|170197231 | 86 | 3 | 21% | Energy metabolism |
| 9 | Phosphatidylethanolamine-binding protein | | ✓ | | 28 | 6.00 | 20.36 | 6.07 | gi\|170189936 | 127 | 3 | 11% | Signaling |
| 10 | Hemocyanin | | | ✓ | 27 | 6.94 | 76.32 | 5.83 | gi\|170187274 | 201 | 5 | 17% | Respiratory |
| 11 | Peroxiredoxin 5 isoform B | | | ✓ | 25 | 6.78 | 19.88 | 8.88 | gi\|170265337 | 205 | 3 | 28% | Signaling |
| 12 | Hemocyanin | | | ✓ | 25 | 6.76 | 76.32 | 5.83 | gi\|170187274 | 275 | 6 | 26% | Respiratory |
| 13 | α/β-Actin | | ✓ | | 23 | 5.78 | 41.91 | 5.16 | gi\|170182624 | 321 | 5 | 24% | Thin filament |
| 17 | Gelsolin | | ✓ | | 18 | 5.67 | 81.77 | 4.79 | gi\|170227754 | 273 | 3 | 20% | Actin-binding |
| 18 | Gelsolin | ✓ | | | 18 | 5.38 | 81.77 | 4.79 | gi\|170227754 | 358 | 4 | 25% | Actin-binding |
| 21 | FK506-binding protein | | | ✓ | 12 | 6.76 | 11.69 | 7.87 | gi\|170246946 | 102 | 1 | 23% | Signaling |
| 22 | Profilin | | | ✓ | 9 | 6.76 | 13.89 | 6.27 | gi\|170182510 | 279 | 4 | 34% | Actin-binding |
| 23 | Arginine kinase | ✓ | | | 46 | 6.66 | 39.96 | 6.05 | gi\|170186144 | 385 | 9 | 35% | Phosphotransfer |
| 25 | Paramyosin | | ✓ | | 16 | 5.94 | 103.02 | 5.46 | isotig00035 | 38 | 2 | 0% | Thick filament |
| 26 | Myosin heavy chain type B | | ✓ | | 14 | 6.09 | 218.87 | 6.00 | gi\|170270277 | 158 | 3 | 13% | Thick filament |
| 27 | Myosin heavy chain type B | | | ✓ | 13 | 6.08 | 218.87 | 6.00 | gi\|170270277 | 100 | 2 | 5% | Thick filament |
| 29 | Cardiac-like muscle actin | ✓ | | | 12 | 6.27 | 41.65 | 5.23 | gi\|170182268 | 172 | 2 | 11% | Thin filament |
| 30 | Prostaglandin reductase | | ✓ | | 19 | 5.84 | 36.49 | 8.31 | gi\|170218863 | 68 | 2 | 7% | Signaling |
| 32 | Phosphohistidine phosphatase 1 | | | ✓ | 11 | 6.39 | 13.82 | 5.34 | gi\|170217426 | 155 | 2 | 13% | Signaling |
| 33 | Cofilin | | | ✓ | 19 | 6.45 | 19.34 | 8.50 | isotig01165 | 201 | 5 | 11% | Actin-binding |
| 34 | α/β-Actin | | | ✓ | 17 | 6.27 | 41.91 | 5.16 | gi\|170182624 | 184 | 4 | 20% | Thin filament |
| 35 | α/β-Actin | | | ✓ | 17 | 6.29 | 41.91 | 5.16 | gi\|170182624 | 193 | 3 | 16% | Thin filament |
| 36 | Glyceraldehyde-3-phosphate dehydrogenase | | ✓ | | 15 | 6.44 | 18.66 | 5.58 | gi\|170197231 | 336 | 5 | 29% | Energy metabolism |
| 37 | Hemocyanin | ✓ | | | 24 | 6.30 | 75.27 | 5.52 | gi\|170187274 | 109 | 2 | 9% | Respiratory |
| 38 | Myosin heavy chain type B | | ✓ | | 16 | 6.10 | 218.87 | 6.00 | gi\|170270277 | 99 | 2 | 5% | Thick filament |
| 39 | α/β-Actin | | | ✓ | 14 | 6.26 | 41.91 | 5.16 | gi\|170182624 | 270 | 3 | 16% | Thin filament |
| 40 | Cardiac-like muscle actin | | ✓ | | 21 | 6.22 | 41.65 | 5.23 | gi\|170182268 | 96 | 2 | 8% | Thin filament |
| 42 | Cardiac-like muscle actin | | | ✓ | 13 | 6.31 | 41.65 | 5.23 | gi\|170182268 | 191 | 2 | 11% | Thin filament |
| 46 | Filamin-A | | | ✓ | 68 | 6.87 | 267.69 | 5.81 | isotig02107 | 54 | 2 | 3% | Actin-binding |
| 49 | Filamin-C | | | ✓ | 63 | 6.68 | 262.65 | 5.90 | gi\|170202097 | 98 | 2 | 8% | Actin-binding |
| 50 | Enolase | | | ✓ | 55 | 6.68 | 39.85 | 5.45 | gi\|170254092 | 181 | 3 | 16% | Energy metabolism |
| 51 | Enolase | | | ✓ | 54 | 6.79 | 47.24 | 6.18 | gi\|170237664 | 202 | 3 | 14% | Energy metabolism |
| 52 | α/β-Actin | | ✓ | | 36 | 5.76 | 41.91 | 5.16 | gi\|170182624 | 390 | 6 | 27% | Thin filament |
| 53 | Myosin regulatory light chain | | ✓ | | 24 | 4.19 | 22.58 | 4.70 | gi\|170184074 | 281 | 5 | 11% | Thick filament |
| 57 | Hemocyanin | | | ✓ | 79 | 6.01 | 75.27 | 5.52 | gi\|170278434 | 153 | 3 | 15% | Respiratory |
| 58 | Hemocyanin | | | ✓ | 78 | 6.06 | 77.54 | 5.37 | gi\|170185161 | 122 | 3 | 14% | Respiratory |
| 59 | Hemocyanin | | | ✓ | 79 | 6.10 | 75.27 | 5.52 | gi\|170278434 | 128 | 2 | 10% | Respiratory |
| 62 | Pseudohemocyanin-1 | | | ✓ | 56 | 5.27 | 79.57 | 5.69 | gi\|170189674 | 60 | 2 | 9% | Respiratory |
| 67 | Proteasome β-subunit type-6-like | | ✓ | | 24 | 6.71 | 25.10 | 5.41 | gi\|170204742 | 46 | 2 | 6% | Signaling |
| 70 | Glyceraldehyde-3-phosphate dehydrogenase | | | ✓ | 15 | 6.79 | 35.54 | 6.54 | gi\|170198680 | 147 | 3 | 15% | Energy metabolism |
| 71 | Myosin heavy chain type B | | | ✓ | 13 | 6.68 | 218.87 | 6.00 | gi\|170270277 | 82 | 2 | 5% | Thick filament |
| 73 | Glyceraldehyde-3-phosphate dehydrogenase | | | ✓ | 17 | 6.52 | 18.66 | 5.58 | gi\|170197231 | 318 | 5 | 29% | Energy metabolism |
| 74 | Glyceraldehyde-3-phosphate dehydrogenase | | | ✓ | 16 | 6.45 | 18.66 | 5.58 | gi\|170197231 | 48 | 2 | 15% | Energy metabolism |
| 75 | Glyceraldehyde-3-phosphate dehydrogenase | | ✓ | | 23 | 6.56 | 18.66 | 5.58 | gi\|170197231 | 253 | 3 | 18% | Energy metabolism |
| 78 | α/β-Actin | | | ✓ | 57 | 4.62 | 41.91 | 5.16 | gi\|170190957 | 77 | 2 | 5% | Thin filament |
| 79 | α/β-Actin | | | ✓ | 51 | 5.28 | 41.91 | 5.16 | gi\|170190957 | 390 | 7 | 21% | Thin filament |
| 80 | α/β-Actin | | | ✓ | 53 | 5.12 | 41.91 | 5.16 | gi\|170190957 | 172 | 4 | 12% | Thin filament |
| 81 | α/β-Actin | | | ✓ | 45 | 4.97 | 41.91 | 5.16 | gi\|170190957 | 439 | 7 | 21% | Thin filament |
| 82 | α/β-Actin | ✓ | | | 54 | 6.64 | 41.91 | 5.16 | gi\|170190957 | 419 | 6 | 18% | Thin filament |
| 83 | Farnesoic acid O-methyltranferase | ✓ | | | 43 | 4.56 | 31.45 | 4.56 | gi\|170188611 | 178 | 3 | 14% | Signaling |
| 84 | α/β-Actin | ✓ | | | 39 | 4.85 | 41.91 | 5.16 | gi\|170190957 | 132 | 2 | 9% | Thin filament |
| 85 | α/β-Actin | | | ✓ | 37 | 4.84 | 41.91 | 5.16 | gi\|170190957 | 400 | 6 | 21% | Thin filament |
| 86 | Sarcomeric α-actinin | ✓ | | | 35 | 4.84 | 97.75 | 6.04 | gi\|170222152 | 132 | 6 | 30% | Actin-binding |
| 87 | Glycogen phosphorylase | | ✓ | | 33 | 5.46 | 97.96 | 6.82 | gi\|170202348 | 147 | 5 | 17% | Energy metabolism |
| 88 | α/β-Actin | | ✓ | | 32 | 5.56 | 41.91 | 5.16 | gi\|170182624 | 210 | 4 | 20% | Thin filament |

**Table S1 continued**

| | | | | | | | | | | | |
|---|---|---|---|---|---|---|---|---|---|---|---|
| 89 | Arginine kinase | | ✓ | 31 | 5.71 | 40.34 | 6.34 | gi\|170183164 | 258 | 5 | 18% | Phosphotransfer |
| 90 | Arginine kinase | | ✓ | 29 | 5.45 | 40.34 | 6.34 | gi\|170183164 | 221 | 5 | 18% | Phosphotransfer |
| 91 | Arginine kinase | | ✓ | 29 | 5.42 | 40.34 | 6.34 | gi\|170183164 | 81 | 2 | 6% | Phosphotransfer |
| 92 | α/β-Actin | | ✓ | 28 | 5.43 | 41.91 | 5.16 | gi\|170182624 | 198 | 4 | 18% | Thin filament |
| 94 | Sarcoplasmic calcium-binding protein | ✓ | | 22 | 4.68 | 21.93 | 4.60 | gi\|170182977 | 168 | 3 | 14% | Signaling |
| 95 | Sarcoplasmic calcium-binding protein | | ✓ | 21 | 4.70 | 21.93 | 4.60 | gi\|170182977 | 161 | 3 | 14% | Signaling |
| 96 | Myosin regulatory light chain | | ✓ | 46 | 6.86 | 22.58 | 4.70 | gi\|170184074 | 273 | 5 | 11% | Thick filament |
| 99 | α/β-Actin | | ✓ | 46 | 5.22 | 41.91 | 5.16 | gi\|170190957 | 257 | 4 | 9% | Thin filament |
| 100 | Arginine kinase | ✓ | | 17 | 5.23 | 46.00 | 4.90 | gi\|170183164 | 283 | 5 | 23% | Phosphotransfer |
| 101 | Arginine kinase | | ✓ | 22 | 5.39 | 46.00 | 4.90 | gi\|170183164 | 202 | 4 | 15% | Phosphotransfer |
| 102 | Arginine kinase | | ✓ | 19 | 5.48 | 46.00 | 4.90 | gi\|170183164 | 135 | 3 | 11% | Phosphotransfer |
| 103 | 14-3-3 ζ | | ✓ | 36 | 4.66 | 27.96 | 4.65 | gi\|170194925 | 42 | 3 | 15% | Signaling |
| 105 | Myosin regulatory light chain | | ✓ | 21 | 4.20 | 22.58 | 4.70 | gi\|170184074 | 206 | 3 | 8% | Thick filament |
| 106 | Glyceraldehyde-3-phosphate dehydrogenase | | ✓ | 40 | 6.88 | 18.66 | 5.58 | gi\|170197231 | 344 | 3 | 24% | Energy metabolism |
| 107 | Arginine kinase | | ✓ | 38 | 6.86 | 46.00 | 4.90 | gi\|170186144 | 263 | 7 | 30% | Phosphotransfer |
| 108 | Arginine kinase | ✓ | | 35 | 6.64 | 46.00 | 4.90 | gi\|170186144 | 457 | 9 | 30% | Phosphotransfer |
| 109 | Arginine kinase | | ✓ | 35 | 6.80 | 46.00 | 4.90 | gi\|170186144 | 241 | 6 | 29% | Phosphotransfer |
| 110 | Arginine kinase | | ✓ | 35 | 6.66 | 46.00 | 4.90 | gi\|170186144 | 386 | 9 | 30% | Phosphotransfer |
| 111 | Arginine kinase | | ✓ | 35 | 6.84 | 46.00 | 4.90 | gi\|170186144 | 153 | 4 | 19% | Phosphotransfer |
| 112 | Triose-phosphate isomerase | | ✓ | 34 | 6.87 | 28.99 | 5.83 | gi\|170207221 | 119 | 3 | 16% | Energy metabolism |
| 113 | Arginine kinase | | ✓ | 33 | 6.79 | 46.00 | 4.90 | gi\|170186144 | 341 | 8 | 34% | Phosphotransfer |
| 114 | Arginine kinase | | ✓ | 33 | 6.63 | 46.00 | 4.90 | gi\|170186144 | 298 | 8 | 30% | Phosphotransfer |
| 115 | Arginine kinase | | ✓ | 31 | 6.63 | 46.00 | 4.90 | gi\|170186144 | 277 | 7 | 29% | Phosphotransfer |
| 116 | Arginine kinase | | ✓ | 40 | 6.81 | 46.00 | 4.90 | gi\|170186144 | 382 | 9 | 30% | Phosphotransfer |
| 118 | Paramyosin | | ✓ | 44 | 6.68 | 103.69 | 5.55 | gi\|170186119 | 142 | 3 | 18% | Thick filament |
| 119 | Muscle myosin heavy chain | | ✓ | 95 | 5.53 | 135.52 | 5.49 | gi\|170208087 | 113 | 3 | 21% | Thick filament |
| 120 | Muscle myosin heavy chain | | ✓ | 95 | 5.49 | 135.52 | 5.49 | gi\|170208087 | 70 | 2 | 10% | Thick filament |
| 123 | Myosin heavy chain type 1 | | ✓ | 75 | 5.50 | 219.58 | 5.76 | gi\|170219699 | 65 | 2 | 10% | Thick filament |
| 125 | Gelsolin-like isoform 1 | | ✓ | 90 | 5.03 | 44.36 | 7.68 | gi\|170227754 | 44 | 2 | 12% | Actin-binding |
| 126 | Muscle myosin heavy chain | | ✓ | 20 | 5.36 | 135.52 | 5.49 | gi\|170208087 | 110 | 3 | 15% | Thick filament |
| 127 | Sarcomeric α-actinin | ✓ | | 63 | 5.21 | 97.75 | 6.04 | gi\|170222152 | 295 | 6 | 30% | Actin-binding |
| 128 | α/β-Actin | | ✓ | 50 | 6.09 | 41.91 | 5.16 | gi\|170190957 | 374 | 6 | 18% | Thin filament |
| 129 | Enolase | | ✓ | 43 | 6.30 | 47.24 | 6.18 | gi\|170237664 | 321 | 7 | 38% | Energy metabolism |
| 130 | Glyceraldehyde-3-phosphate dehydrogenase | | ✓ | 40 | 6.56 | 18.66 | 5.58 | gi\|170197231 | 348 | 4 | 24% | Energy metabolism |
| 131 | Fast myosin heavy chain | | ✓ | 41 | 6.40 | 47.85 | 5.24 | gi\|170220415 | 146 | 2 | 26% | Thick filament |
| 132 | α/β-Actin | | ✓ | 53 | 6.11 | 41.91 | 5.16 | gi\|170190957 | 400 | 7 | 21% | Thin filament |
| 133 | Troponin T | | ✓ | 53 | 6.15 | 45.88 | 4.97 | gi\|170228768 | 120 | 2 | 15% | Thin filament |
| 134 | Arginine kinase | ✓ | | 37 | 6.63 | 46.00 | 4.90 | gi\|170186144 | 366 | 9 | 30% | Phosphotransfer |
| 135 | α/β-Actin | | ✓ | 50 | 6.27 | 41.91 | 5.16 | gi\|170190957 | 226 | 5 | 12% | Thin filament |
| 136 | α/β-Actin | | ✓ | 50 | 6.19 | 41.91 | 5.16 | gi\|170190957 | 388 | 6 | 18% | Thin filament |
| 137 | Pyruvate dehydrogenase E1 α-subunit | | ✓ | 45 | 6.23 | 43.20 | 7.58 | gi\|170183821 | 49 | 2 | 10% | Energy metabolism |
| 138 | Hemocyanin | | ✓ | 45 | 6.28 | 75.27 | 5.52 | gi\|170187274 | 209 | 4 | 18% | Respiratory |
| 139 | Notch-type protein | | ✓ | 67 | 6.62 | 44.88 | 7.22 | gi\|170248782 | 130 | 6 | 28% | Signaling |
| 141 | Filamin-C | | ✓ | 66 | 6.53 | 249.86 | 6.12 | gi\|170202097 | 80 | 2 | 9% | Actin-binding |
| 142 | Filamin-A | | ✓ | 61 | 6.65 | 287.86 | 6.61 | gi\|170203114 | 76 | 2 | 8% | Actin-binding |
| 143 | Phosphoglycerate kinase-like | | ✓ | 54 | 6.61 | 53.54 | 9.17 | gi\|170203088 | 229 | 6 | 27% | Energy metabolism |
| 145 | Arginine kinase | ✓ | | 46 | 6.57 | 46.00 | 4.90 | gi\|170186144 | 151 | 4 | 16% | Phosphotransfer |
| 146 | Filamin | ✓ | | 83 | 6.82 | 249.86 | 6.12 | gi\|170220786 | 86 | 2 | 11% | Actin-binding |
| 148 | Cardiac-like muscle actin | | ✓ | 53 | 6.21 | 41.65 | 5.23 | gi\|170182268 | 169 | 2 | 11% | Thin filament |
| 149 | Enolase | ✓ | | 53 | 6.72 | 39.85 | 5.45 | gi\|170254092 | 161 | 4 | 19% | Energy metabolism |
| 150 | Cardiac-like muscle actin | | ✓ | 41 | 5.75 | 41.65 | 5.23 | gi\|170182268 | 162 | 3 | 14% | Thin filament |
| 153 | Arginine kinase | ✓ | | 31 | 5.93 | 46.00 | 4.90 | gi\|170186144 | 264 | 7 | 33% | Phosphotransfer |
| 154 | Arginine kinase | ✓ | | 32 | 6.86 | 46.00 | 4.90 | gi\|170200859 | 391 | 8 | 29% | Phosphotransfer |
| 155 | Triose-phopshate isomerase | | ✓ | 31 | 6.85 | 26.98 | 5.87 | gi\|170254610 | 233 | 4 | 26% | Energy metabolism |
| 156 | Arginine kinase | | ✓ | 29 | 6.17 | 46.00 | 4.90 | gi\|170186144 | 88 | 3 | 14% | Phosphotransfer |
| 157 | Troponin T | | ✓ | 28 | 5.82 | 45.58 | 4.97 | gi\|170228768 | 96 | 2 | 11% | Thin filament |
| 158 | Adendylate kinase | | ✓ | 28 | 6.65 | 29.30 | 8.05 | gi\|170218197 | 502 | 8 | 27% | Phosphotransfer |
| 159 | Arginine kinase | ✓ | | 28 | 5.65 | 46.00 | 4.90 | gi\|170183164 | 137 | 3 | 9% | Phosphotransfer |
| 160 | Hemocyanin subunit 1 | ✓ | | 27 | 6.15 | 25.41 | 5.99 | gi\|170195414 | 168 | 4 | 17% | Respiratory |
| 161 | α/β-Actin | | ✓ | 25 | 5.77 | 41.91 | 5.16 | gi\|170182624 | 217 | 4 | 20% | Thin filament |

**Table S1 continued**

| | | | | | | | | | | | |
|---|---|---|---|---|---|---|---|---|---|---|---|
| 162 | Arginine kinase | | ✓ | 22 | 5.60 | 46.00 | 4.90 | gi\|170183164 | 206 | 4 | 9% | Phosphotransfer |
| 163 | Arginine kinase | ✓ | | 21 | 5.57 | 46.00 | 4.90 | gi\|170183164 | 353 | 5 | 21% | Phosphotransfer |
| 164 | Myosin regulatory light chain | | ✓ | 21 | 4.14 | 22.58 | 4.70 | gi\|170184074 | 176 | 3 | 8% | Thick filament |
| 165 | Arginine kinase | | ✓ | 20 | 5.21 | 46.00 | 4.90 | gi\|170183164 | 62 | 2 | 6% | Phosphotransfer |
| 167 | Glyceraldehyde-3-phosphate dehydrogenase | ✓ | | 20 | 6.55 | 18.66 | 5.58 | gi\|170197231 | 172 | 3 | 21% | Energy metabolism |
| 168 | Troponin T | | ✓ | 52 | 6.80 | 45.88 | 4.97 | gi\|170228768 | 45 | 2 | 8% | Thin filament |
| 178 | Slow muscle myosin S1 heavy chain | | ✓ | 66 | 5.51 | 58.53 | 5.22 | gi\|170194515 | 148 | 4 | 14% | Thick filament |
| 179 | Hemocyanin subunit 4 | | ✓ | 65 | 5.47 | 77.04 | 5.30 | gi\|170214816 | 96 | 3 | 13% | Respiratory |
| 180 | α/β-Actin | | ✓ | 53 | 4.91 | 41.91 | 5.16 | gi\|170190957 | 223 | 6 | 18% | Thin filament |
| 183 | Arginine kinase | | ✓ | 29 | 5.69 | 46.00 | 4.90 | gi\|170183164 | 373 | 5 | 22% | Phosphotransfer |
| 184 | Arginine kinase | | ✓ | 23 | 5.17 | 46.00 | 4.90 | gi\|170183164 | 90 | 3 | 10% | Phosphotransfer |
| 185 | α/β-Actin | | ✓ | 20 | 5.10 | 41.91 | 5.16 | gi\|170190957 | 151 | 4 | 6% | Thin filament |
| 187 | Hemocyanin | | ✓ | 24 | 6.75 | 75.27 | 5.52 | gi\|170187274 | 215 | 5 | 17% | Respiratory |
| 189 | Paramyosin (long form) | ✓ | | 67 | 6.19 | 103.02 | 5.83 | isotig00035 | 62 | 2 | 0% | Thick filament |
| 192 | Tropomyosin (slow muscle isoform) | | ✓ | 47 | 4.48 | 32.89 | 4.74 | gi\|170187278 | 348 | 7 | 26% | Thin filament |
| 193 | F1-ATP synthase β-subunit | ✓ | | 68 | 6.13 | 55.80 | 5.31 | gi\|170221081 | 361 | 7 | 33% | Energy metabolism |
| 194 | Myosin heavy chain type 1 | | ✓ | 81 | 5.55 | 219.58 | 5.76 | gi\|170219699 | 64 | 2 | 10% | Thick filament |
| 198 | Myosin regulatory light chain | | ✓ | 20 | 4.12 | 22.58 | 4.70 | gi\|170184074 | 311 | 6 | 14% | Thick filament |
| 200 | Myosin heavy chain type 1 | | ✓ | 95 | 5.63 | 219.58 | 5.76 | gi\|170219699 | 100 | 2 | 9% | Thick filament |
| 203 | α/β-Actin | | ✓ | 50 | 5.90 | 41.91 | 5.16 | gi\|170190957 | 380 | 6 | 18% | Thin filament |
| 204 | Tropomyosin (slow muscle isoform) | | ✓ | 47 | 4.51 | 32.89 | 4.74 | gi\|170187278 | 407 | 8 | 27% | Thin filament |
| 320 | Fructose 1,6-bisphosphate aldolase | ✓ | | 15 | 5.44 | 25.64 | 5.47 | gi\|170216091 | 287 | 5 | 31% | Energy metabolism |
| 387 | α/β-Actin | | ✓ | 58 | 5.28 | 41.91 | 5.16 | gi\|170190957 | 193 | 6 | 15% | Thin filament |
| 439 | Myosin heavy chain type B | ✓ | | 108 | 6.10 | 218.87 | 6.00 | gi\|170211824 | 42 | 2 | 8% | Thick filament |